TNFR1 (hTNFR1, 16.0×10^{-4} s^{-1}; mTNFR1, 37.0×10^{-4} s^{-1}) were clearly higher than those of the wtTNF (hTNFR1, 3.0×10^{-4} s^{-1}; mTNFR1, 1.5×10^{-4} s^{-1}). The association kinetic constants (k_{on}) of the R1antTNF for the human and mouse TNFR1 were also higher than those of the wtTNF. These results suggest that the R1antTNF interacts with the TNFR1 by repeating very quick binding and dissociation, and has a binding mode that is different from that of the wtTNF.

TABLE 4
X-ray data collection and refinement statistics (molecular replacement)

Crystal	R1antTNF
Data collection	
Space group	$P2_12_12_1$
Cell dimensions	
a, *b*, *c* (Å)	66.56, 66.97, 103.56
Resolution (Å)	50.0-1.80 (1.86-1.80)[a]
R_{merge}	0.063 (0.484)
$I/\sigma I$	36.8 (2.71)
Completeness (%)	99.6 (96.1)
Redundancy	7.1 (6.0)
Refinement	
Resolution (Å)	41.0-1.80
No. of reflections	42,155
R_{work}/R_{free}	19.8/23.9
No. of atoms	
Protein	3384
Water	237
Root mean squares deviations	
Bond lengths (Å)	0.00840
Bond angles (°)	1.47

[a] Highest resolution shell is shown in parentheses.

Crystal Structure of R1antTNF—To understand the structural basis for the different binding mode and absence of signal transduction via the R1antTNF, we examined the structure of R1antTNF by x-ray crystallography. After establishing crystallization conditions, good quality crystals of R1antTNF were obtained. The R1antTNF crystal size was ~$0.2 \times 0.2 \times 0.4$ mm^3. X-ray diffraction data were collected in SPring-8 (the large synchrotron radiation facility in Japan). Analysis of these data show that the space group is $P2_12_12_1$, and the lattice constants are $a = 64.56$, $b = 66.97$, and $c = 103.56$ Å (Table 4). The R1antTNF structure was further refined using CNS. Results of the model validation using the Procheck were as follows: 88.4% residues in the most favored regions; 11.0% residues in the additional allowed regions; 0.6% residues in the generously allowed regions; and 0.0% residues in the disallowed regions. The overall structure of the R1antTNF was a trimer (Fig. 6*A*) (PDB code 2E7A), which was similar to that of the wtTNF trimer (Fig. 6*B*) (PDB code 1TNF) (37). Interestingly, structural superposition of the R1antTNF and human wtTNF showed extraordinary similarity (root mean square deviation 1.17 Å for 444 C-α atoms) of their overall structures despite their contradictory functions (Fig. 6*C*). It is believed that the TNF signaling is initiated by the formation of a complex with the three TNFRs on the cell surface. However, the fact that the R1antTNF did not transduce signaling suggests that there might be other structural differences between the wtTNF and R1antTNF.

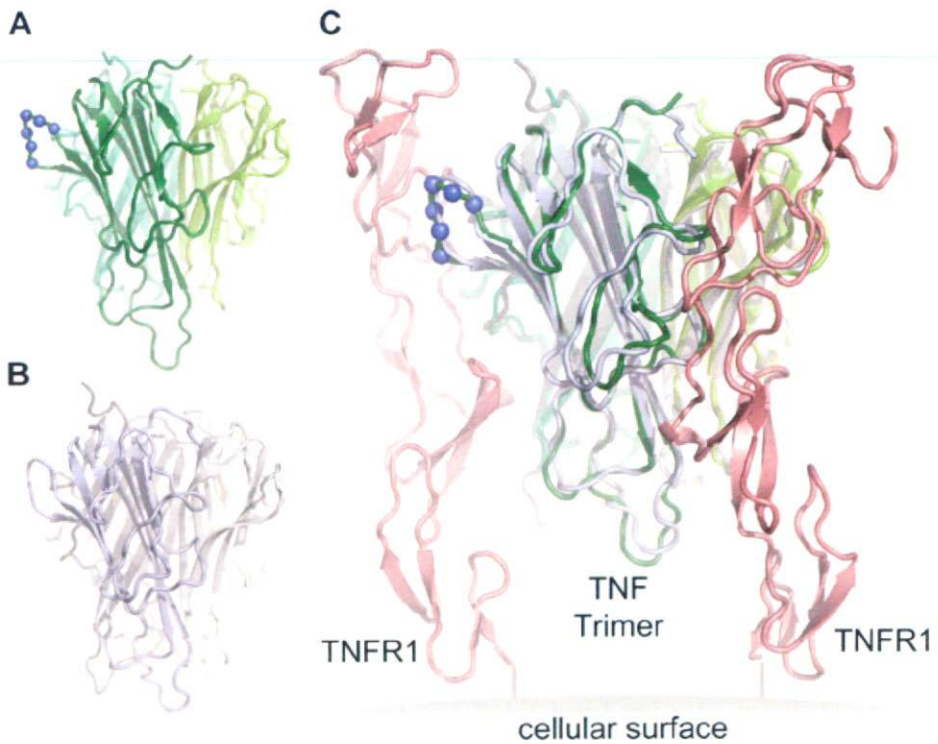

FIGURE 6. **Overall structures of R1antTNF and wtTNF.** *A*, refined structure of the R1antTNF trimer (*green*). *Blue spheres* show the mutated residues(amino acids 84–89) in R1antTNF. This structure is registered in the PDB (PDB code 2E7A). *B*, structure of the wtTNF trimer (*gray*). This structure has been published, and its PDB code is 1TNF. *C*, model structures of the TNF-TNFR1 complexes. Each TNF is superposed on the LT-α derived from the LT-α-TNFR1 complex (PDB code 1TNR). TNF binds to three R1 monomers on the cell surface. TNFR1s are shown using *red schematics*. Superposition of the structures of the wtTNF and R1antTNF was performed using the ccp4i program.

DISCUSSION

TNF, secreted from the site of injury or because of the activation of the immune cells, is involved in the development of inflammatory diseases, and it predominantly activates TNFR1 (40, 41). The TNFR1 knock-out mice have been reported to be resistant to the onset of several inflammatory diseases, such as sepsis, rheumatoid arthritis, and multiple sclerosis (14, 16, 42). In agreement with this, blocking the interaction between the TNF and TNFR1 has emerged as a powerful and clinically effective therapy for the acute inflammation and autoimmune conditions. In this study, we generated TNFR1-selective antagonistic TNF mutants using a phage library displaying structural variants of human TNF.

Among 10 potential candidates, the mutTNF-T2 (R1antTNF) selectively and strongly bound to the TNFR1 but showed almost no bioactivity. Additionally, we found that R1antTNF most effectively inhibited the wtTNF-induced cell death

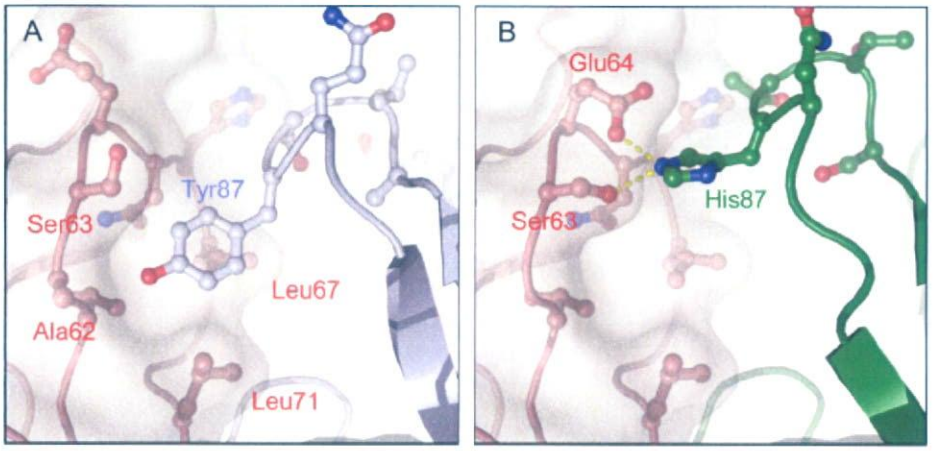

FIGURE 7. **Structural difference between the receptor binding region of the R1antTNF and wtTNF.** *A*, interaction between the wtTNF (*gray*) and TNFR1 (*red*). *White layer* depicts the molecular surface of the TNFR1. Hydrophobic interaction is formed between the Tyr-87 and molecular pocket in the TNFR1 (Leu-67, Leu-71, Ala-62, and Ser-63). *B*, interaction between the R1antTNF (*green*) and TNFR1 (*red*). *Yellow broken lines* show the possible interactions of the R1antTNF His-87 with the receptor Ser-63 and Glu-64. In this simulation, the side chains of each structure were rotated to fit the predicted interaction. Stable structures of these rotamers were constructed using the O program.

(Fig. 3*B*). R1antTNF also clearly inhibited the TNF functions other than cytotoxicity. Interestingly, the ratio between the R1antTNF and wtTNF was 1000-fold or more to obtain 50% inhibition against the wtTNF-induced cytotoxicity and caspase-3/7 activity, whereas the ratio was only about 100-fold or less to obtain 50% inhibition against the wtTNF-induced expression of E-selectin, production of GM-CSF, and NF-κB activation. Intracellular signaling induced by the TNF/TNFR1 interaction is divided into the following two main pathways: (i) the NF-κB pathway, which regulates the expression of adhesion molecules and inflammatory cytokines, and (ii) the caspase cascade, which induces cell death through apoptosis or necrosis (34). Our results suggest that R1antTNF is more antagonistic against the wtTNF function mediated via the NF-κB pathway than via the caspase cascade. In pathological tissues, endogenous TNF induced expression of the cell adhesion molecules and inflammatory cytokines resulting in leukocyte infiltration, which are regulated by NF-κB and are closely related to the development or exacerbation of diseases (43) such as fulminant hepatitis and rheumatoid arthritis. Because the R1antTNF efficiently inhibited the TNF-induced NF-κB activation, it would be of therapeutic value for the treatment of such inflammatory diseases. These cell line or signaling pathway-dependent differences in the inhibitory efficiencies of R1antTNF could be valuable in studying the structural or biological changes caused by the TNF/TNFR1 interactions, which need to be explored further.

We examined the therapeutic effects of R1antTNF in the acute lethal hepatitis model. R1antTNF exhibited the suppressive effect on acute hepatitis. Although the R1antTNF suppressed the elevation of the ALT level in a dose-dependent manner, the survival rate was not significantly improved between the dose 10 μg/mouse *versus* 270 μg/mouse. This discrepancy is likely because the difference in the degree of suppression of the elevated ALT level does not always correlate well with the improvement in the survival rate. Nevertheless, treatment with only 30–270 μg/mouse R1antTNF (30–270-fold excess over wtTNF) significantly suppressed the elevation of ALT levels and reduced the lethal toxicity. Thus, the antagonistic activity of R1antTNF *in vivo* was stronger than expected from the *in vitro* results. The TNF/GalN-mediated activation of TNFR1 not only induces apoptosis and necrosis of hepatocytes but also induces inflammatory responses and secondary responses associated with the cell death (44). Therefore, we believe that the R1antTNF exerted its therapeutic effect by comprehensively inhibiting the TNF/GalN-mediated biological responses, thus blocking the liver failure in the experimental animals. The R1antTNF is also expected to have therapeutic effect in chronic inflammatory disease models, such as in collagen-induced arthritis model and experimental autoimmune encephalomyelitis model. However, the plasma half-life of R1antTNF, like the wtTNF, is very short (12 min). We recently developed a novel PEGylation system that dramatically improved the *in vivo* stability and therapeutic effects of the bioactive proteins (29, 45). We are currently in the process of developing the PEGylated R1antTNF to further enhance its potential anti-inflammatory activity.

To explore the underlying mechanism of the antagonistic activity of R1antTNF, we examined the crystal structure of R1antTNF by x-ray crystallography. Despite close resemblance between the crystal structure of the R1antTNF and wtTNF, the receptor-bound R1antTNF did not transmit any signal via the TNFR1. To further speculate why the R1antTNF showed antagonistic activity, we utilized the superpose program to perform docking simulations with the TNFs and TNFR1 using the crystal structure of the LT-α-TNFR1 complex (PDB code 1TNR) (31). The TNF-TNFR1 model complex suggested that the Tyr-87 of the wtTNF, an essential residue, is buried in a molecular hydrophobic "pocket" of the TNFR1, which houses the receptor residues Leu-67 and Leu-71 that are implicated to maintain the TNF and TNFR1 complex (Fig. 7*A*). Tyr-87 is a highly conserved residue throughout the TNF superfamily, such as LT-α, LT-β and LIGHT, and this discussion is also reflected in the crystal structure of the LT-α-TNFR1 complex (38). Accordingly, site-directed mutagenesis of the Tyr-87 residue of TNF resulted in a dramatic loss of its biological activity and affinities for both TNFRs (39), suggesting that this residue is be essential for TNF function. However, in R1antTNF, the Tyr-87 is replaced with a histidine residue. The structural simulation studies suggested that the His-87 in R1antTNF could interact with the relatively negatively charged Ser-63 and Glu-64 residues on the TNFR1 surface, which probably explains the different binding mode of the R1antTNF as compared with the wtTNF (Fig. 7*B*).

Indeed, the association and dissociation kinetic constants (k_{on} and k_{off}, respectively) for the binding of R1antTNF to TNFR1 were considerably higher than those of the wtTNF, indicating a difference in the TNFR1-binding pattern between the wtTNF and R1antTNF (Table 3). The association and dissociation kinetic constants are very important factors in discussing the ligand-receptor interaction and function. It was previously shown that the membrane-bound TNF, but not the soluble TNF, could activate the TNFR2, and the reason for this difference was attributed to the dissociation kinetic constant of the soluble TNF, which was much higher than the membrane-bound TNF (46). Therefore, the inability of R1antTNF to transmit signal and its antagonistic activity are probably because of the higher k_{on} and k_{off} values of R1antTNF for the TNFR1, suggesting that they influenced the stability of the TNF-TNFR1 complex and reduced the continuous binding time required for the signal transmission. In addition, we demonstrated that R1antTNF inhibited the activations of both caspase-3/7 and NF-κB (Fig. 5, *A* and *B*), which are mediated via two distinct intracellular signaling complexes. TNF/TNFR1-mediated signaling requires sequential formation of the following two receptor complexes: the complex I is involved in the recruitment of TRADD, RIP1, and TRAF2 leading to the NF-κB activation, whereas the consequent complex II is involved in internalization, post-translational modifications, and recruitment of FADD and caspase-8 initiating apoptosis (47). Together, these results suggest that R1antTNF blocked the TNF-mediated signal transmission by binding to TNFR1 in a rapid association/dissociation cycle, thereby inhibiting the formation of the intracellular complexes. However, more detailed investigations, such as detection of these intracellular complexes and their internalization, other TNF/TNFR1-mediated signaling, and analysis of the complex structure of the R1antTNF and TNFR1, are required to elucidate exactly how the R1antTNF exhibits its TNFR1 antagonistic activity.

We succeeded in developing the first mutant form of the human TNF with TNFR1-selective antagonistic activity by using a unique combinatorial phage-based technique. Existing TNF blockers, *i.e.* etanercept and infliximab, are widely used in the treatment of rheumatoid arthritis and Crohn disease (5). But these drugs, which prevent TNF binding on both TNF receptor types, can cause serious side effects, such as mycobacterial infections and hepatitis B virus infection (48). Although TNFR1 is believed to be important for immunological responses (42), TNFR2 is thought to be also important for antiviral resistance and is effective for controlling the mycobacterial infection by affecting the membrane-bound TNF stimulation (18, 49). Therefore, this mutant TNF, R1antTNF, might be a new therapeutic drug with reduced side effects. We are currently evaluating not only the therapeutic effect of R1antTNF on rheumatoid arthritis or experimental encephalomyelitis model, and but also its side effects such as mycobacterial and virus infection. Finally, our studies demonstrate the feasibility of generating TNF receptor subtype-selective antagonistic mutants by comprehensive substitution of sets of amino acids in the wild-type ligand proteins. Our data also suggest that this combinatorial biosynthetic strategy using the bioactive protein as the "lead protein" is very effective in creating receptor-specific agonists and antagonists, and we believe that this approach will generate protein drugs of improved therapeutic value.

Acknowledgment—We thank E. C. Gabazza for discussions and critical reading of the manuscript.

REFERENCES

1. Aggarwal, B. B. (2003) *Nat. Rev. Immunol.* **3,** 745–756
2. Aderka, D., Engelmann, H., Maor, Y., Brakebusch, C., and Wallach, D. (1992) *J. Exp. Med.* **175,** 323–329
3. Feldmann, M., and Maini, R. N. (2003) *Nat. Med.* **9,** 1245–1250
4. Muto, Y., Nouri-Aria, K. T., Meager, A., Alexander, G. J., Eddleston, A. L., and Williams, R. (1988) *Lancet* **2,** 72–74
5. Feldmann, M. (2002) *Nat. Rev. Immunol.* **2,** 364–371
6. Goldbach-Mansky, R., and Lipsky, P. E. (2003) *Annu. Rev. Med.* **54,** 197–216
7. Brown, S. L., Greene, M. H., Gershon, S. K., Edwards, E. T., and Braun, M. M. (2002) *Arthritis Rheum.* **46,** 3151–3158
8. Keane, J., Gershon, S., Wise, R. P., Mirabile-Levens, E., Kasznica, J., Schwieterman, W. D., Siegel, J. N., and Braun, M. M. (2001) *N. Engl. J. Med.* **345,** 1098–1104
9. Nathan, D. M., Angus, P. W., and Gibson, P. R. (2006) *J. Gastroenterol. Hepatol.* **21,** 1366–1371
10. Shakoor, N., Michalska, M., Harris, C. A., and Block, J. A. (2002) *Lancet* **359,** 579–580
11. Sicotte, N. L., and Voskuhl, R. R. (2001) *Neurology* **57,** 1885–1888
12. Aggarwal, B. B., Eessalu, T. E., and Hass, P. E. (1985) *Nature* **318,** 665–667
13. Leist, M., Gantner, F., Jilg, S., and Wendel, A. (1995) *J. Immunol.* **154,** 1307–1316
14. Mori, L., Iselin, S., De Libero, G., and Lesslauer, W. (1996) *J. Immunol.* **157,** 3178–3182
15. Liu, J., Marino, M. W., Wong, G., Grail, D., Dunn, A., Bettadapura, J., Slavin, A. J., Old, L., and Bernard, C. C. (1998) *Nat. Med.* **4,** 78–83
16. Kassiotis, G., and Kollias, G. (2001) *J. Exp. Med.* **193,** 427–434
17. Fremond, C., Allie, N., Dambuza, I., Grivennikov, S. I., Yeremeev, V., Quesniaux, V. F., Jacobs, M., and Ryffel, B. (2005) *Respir. Res.* **6,** 136
18. Olleros, M. L., Guler, R., Corazza, N., Vesin, D., Eugster, H. P., Marchal, G., Chavarot, P., Mueller, C., and Garcia, I. (2002) *J. Immunol.* **168,** 3394–3401
19. Grell, M., Becke, F. M., Wajant, H., Mannel, D. N., and Scheurich, P. (1998) *Eur. J. Immunol.* **28,** 257–263
20. Kafrouni, M. I., Brown, G. R., and Thiele, D. L. (2003) *J. Leukocyte Biol.* **74,** 564–571
21. Kim, E. Y., Priatel, J. J., Teh, S. J., and Teh, H. S. (2006) *J. Immunol.* **176,** 1026–1035
22. Engelmann, H., Holtmann, H., Brakebusch, C., Avni, Y. S., Sarov, I., Nophar, Y., Hadas, E., Leitner, O., and Wallach, D. (1990) *J. Biol. Chem.* **265,** 14497–14504
23. Carter, P. H., Scherle, P. A., Muckelbauer, J. K., Voss, M. E., Liu, R. Q., Thompson, L. A., Tebben, A. J., Solomon, K. A., Lo, Y. C., Li, Z., Strzemienski, P., Yang, G., Falahatpisheh, N., Xu, M., Wu, Z., Farrow, N. A., Ramnarayan, K., Wang, J., Rideout, D., Yalamoori, V., Domaille, P., Underwood, D. J., Trzaskos, J. M., Friedman, S. M., Newton, R. C., and Decicco, C. P. (2001) *Proc. Natl. Acad. Sci. U. S. A.* **98,** 11879–11884
24. Murali, R., Cheng, X., Berezov, A., Du, X., Schon, A., Freire, E., Xu, X., Chen, Y. H., and Greene, M. I. (2005) *Proc. Natl. Acad. Sci. U. S. A.* **102,** 10970–10975
25. Vandenabeele, P., Declercq, W., Vercammen, D., Van de Craen, M., Grooten, J., Loetscher, H., Brockhaus, M., Lesslauer, W., and Fiers, W. (1992) *J. Exp. Med.* **176,** 1015–1024
26. Tsutsumi, Y., Kihira, T., Tsunoda, S., Kanamori, T., Nakagawa, S., and Mayumi, T. (1995) *Br. J. Cancer* **71,** 963–968
27. Barbara, J. A., Smith, W. B., Gamble, J. R., Van Ostade, X., Vandenabeele,

P., Tavernier, J., Fiers, W., Vadas, M. A., and Lopez, A. F. (1994) *EMBO J.* **13,** 843–850
28. Brunetti, C. R., Paulose-Murphy, M., Singh, R., Qin, J., Barrett, J. W., Tardivel, A., Schneider, P., Essani, K., and McFadden, G. (2003) *Proc. Natl. Acad. Sci. U. S. A.* **100,** 4831–4836
29. Yamamoto, Y., Tsutsumi, Y., Yoshioka, Y., Nishibata, T., Kobayashi, K., Okamoto, T., Mukai, Y., Shimizu, T., Nakagawa, S., Nagata, S., and Mayumi, T. (2003) *Nat. Biotechnol.* **21,** 546–552
30. Potterton, E., Briggs, P., Turkenburg, M., and Dodson, E. (2003) *Acta Crystallogr. Sect. D. Biol. Crystallogr.* **59,** 1131–1137
31. Banner, D. W., D'Arcy, A., Janes, W., Gentz, R., Schoenfeld, H. J., Broger, C., Loetscher, H., and Lesslauer, W. (1993) *Cell* **73,** 431–445
32. Jones, T. A., Zou, J. Y., Cowan, S. W., and Kjeldgaard, M. (1991) *Acta Crystallogr. Sect. A.* **47,** 110–119
33. Brunger, A. T., Adams, P. D., Clore, G. M., DeLano, W. L., Gros, P., Grosse-Kunstleve, R. W., Jiang, J. S., Kuszewski, J., Nilges, M., Pannu, N. S., Read, R. J., Rice, L. M., Simonson, T., and Warren, G. L. (1998) *Acta Crystallogr. Sect. D. Biol. Crystallogr.* **54,** 905–921
34. Chen, G., and Goeddel, D. V. (2002) *Science* **296,** 1634–1635
35. Mackay, F., Loetscher, H., Stueber, D., Gehr, G., and Lesslauer, W. (1993) *J. Exp. Med.* **177,** 1277–1286
36. Hishinuma, I., Nagakawa, J., Hirota, K., Miyamoto, K., Tsukidate, K., Yamanaka, T., Katayama, K., and Yamatsu, I. (1990) *Hepatology* **12,** 1187–1191
37. Eck, M. J., and Sprang, S. R. (1989) *J. Biol. Chem.* **264,** 17595–17605
38. Harrop, J. A., McDonnell, P. C., Brigham-Burke, M., Lyn, S. D., Minton, J., Tan, K. B., Dede, K., Spampanato, J., Silverman, C., Hensley, P., DiPrinzio, R., Emery, J. G., Deen, K., Eichman, C., Chabot-Fletcher, M., Truneh, A., and Young, P. R. (1998) *J. Biol. Chem.* **273,** 27548–27556
39. Zhang, X. M., Weber, I., and Chen, M. J. (1992) *J. Biol. Chem.* **267,** 24069–24075
40. Ruuls, S. R., Hoek, R. M., Ngo, V. N., McNeil, T., Lucian, L. A., Janatpour, M. J., Korner, H., Scheerens, H., Hessel, E. M., Cyster, J. G., McEvoy, L. M., and Sedgwick, J. D. (2001) *Immunity* **15,** 533–543
41. Grell, M., Douni, E., Wajant, H., Lohden, M., Clauss, M., Maxeiner, B., Georgopoulos, S., Lesslauer, W., Kollias, G., Pfizenmaier, K., and Scheurich, P. (1995) *Cell* **83,** 793–802
42. Rothe, J., Lesslauer, W., Lotscher, H., Lang, Y., Koebel, P., Kontgen, F., Althage, A., Zinkernagel, R., Steinmetz, M., and Bluethmann, H. (1993) *Nature* **364,** 798–802
43. Zhou, A., Scoggin, S., Gaynor, R. B., and Williams, N. S. (2003) *Oncogene* **22,** 2054–2064
44. Nagaki, M., Sugiyama, A., Osawa, Y., Naiki, T., Nakashima, S., Nozawa, Y., and Moriwaki, H. (1999) *J. Hepatol.* **31,** 997–1005
45. Kamada, H., Tsutsumi, Y., Sato-Kamada, K., Yamamoto, Y., Yoshioka, Y., Okamoto, T., Nakagawa, S., Nagata, S., and Mayumi, T. (2003) *Nat. Biotechnol.* **21,** 399–404
46. Krippner-Heidenreich, A., Tubing, F., Bryde, S., Willi, S., Zimmermann, G., and Scheurich, P. (2002) *J. Biol. Chem.* **277,** 44155–44163
47. Micheau, O., and Tschopp, J. (2003) *Cell* **114,** 181–190
48. Gomez-Reino, J. J., Carmona, L., Valverde, V. R., Mola, E. M., and Montero, M. D. (2003) *Arthritis Rheum.* **48,** 2122–2127
49. Saunders, B. M., Tran, S., Ruuls, S., Sedgwick, J. D., Briscoe, H., and Britton, W. J. (2005) *J. Immunol.* **174,** 4852–4859

British Journal of Pharmacology (2008), 1–10

0007–1188/08 $30.00
www.brjpharmacol.org

RESEARCH PAPER

Comparative study on transduction and toxicity of protein transduction domains

T Sugita[1,2], T Yoshikawa[1], Y Mukai[1,2], N Yamanada[1,2], S Imai[1,2], K Nagano[1,2], Y Yoshida[1,3], H Shibata[1], Y Yoshioka[1,4], S Nakagawa[2], H Kamada[1,4], S-i Tsunoda[1,4] and Y Tsutsumi[1,3,4]

[1]*Laboratory of Pharmaceutical Proteomics, National Institute of Biomedical Innovation (NIBIO), Ibaraki, Osaka, Japan;* [2]*Department of Biotechnology and Therapeutics, Graduate School of Pharmaceutical Sciences, Osaka University, Suita, Osaka, Japan;* [3]*Department of Biomedical Innovation, Graduate School of Pharmaceutical Sciences, Osaka University, Suita, Osaka, Japan and* [4]*The Center for Advanced Medical Engineering and Informatics, Osaka University, Suita, Osaka, Japan*

Background and purpose: Protein transduction domains (PTDs), such as Tat, antennapedia homeoprotein (Antp), Rev and VP22, have been extensively utilized for intracellular delivery of biologically active macromolecules *in vitro* and *in vivo*. There is little known, however, about the relative transduction efficacy, cytotoxicity and internalization mechanism of individual PTDs.
Experimental approach: We examined the cargo delivery efficacies of four major PTDs (Tat, Antp, Rev and VP22) and evaluated their toxicities and cell internalizing pathways in various cell lines.
Key results: The relative order of the transduction efficacy of these PTDs conjugated to fluorescein was Rev > Antp > Tat > VP22, independent of cell type (HeLa, HaCaT, A431, Jurkat, MOLT-4 and HL60 cells). Antp produced significant toxicity in HeLa and Jurkat cells, and Rev produced significant toxicity in Jurkat cells. Flow cytometric analysis demonstrated that the uptake of PTD–fluorescein conjugate was dose-dependently inhibited by methyl-β-cyclodextrin, cytochalasin D and amiloride, indicating that all four PTDs were internalized by the macropinocytotic pathway. Accordingly, in cells co-treated with 'Tat-fused' endosome-disruptive HA2 peptides (HA2-Tat) and independent PTD-fluorescent protein conjugates, fluorescence spread throughout the cytosol, indicating that all four PTDs were internalized into the same vesicles as Tat.
Conclusions and implications: These findings suggest that macropinocytosis-dependent internalization is a crucial step in PTD-mediated molecular transduction. From the viewpoint of developing effective and safe protein transduction technology, although Tat was the most versatile carrier among the peptides studied, PTDs should be selected based on their individual characteristics.
British Journal of Pharmacology advance online publication, 28 January 2008; doi:10.1038/sj.bjp.0707678

Keywords: protein transduction domains; Tat; antennapedia; Rev; VP22; macropinocytosis

Abbreviations: PTD, protein transduction domain; Antp, antennapedia

Introduction

A strong focus of research in the post-genomic era is the development of effective therapies for refractory diseases such as cancer and neurodegenerative syndromes (Rhodes and Chinnaiyan, 2005; Brusic *et al.*, 2007; Drabik *et al.*, 2007). Because the therapeutic targets of these diseases generally exist inside the cell, it is necessary to establish drug delivery methods that transfer macromolecules, such as therapeutic proteins or peptide-based drugs, across the cellular membrane (Nori and Kopecek, 2005; Murriel and Dowdy, 2006; Borsello and Forloni, 2007).

Correspondence: Dr S-i Tsunoda, Laboratory of Pharmaceutical Proteomics, National Institute of Biomedical Innovation (NIBIO), 7-6-8 Saito-Asagi, Ibaraki, Osaka 597-0085, Japan.
E-mail: tsunoda@nibio.go.jp
Received 9 November 2007; accepted 4 December 2007

Protein transduction is a recently developed method for delivering biologically active proteins directly into mammalian cells with high efficiency (Hawiger, 1999; Schwarze *et al.*, 2000). Recombinant technology is used to modify the biophysical properties of proteins and peptides, particularly with respect to their cell permeability, using the so-called protein transduction domains (PTDs) (Nagahara *et al.*, 1998; Rojas *et al.*, 1998; Schwarze *et al.*, 1999). The HIV-1-derived Tat peptide renders various macromolecules cell permeable. Although the initial reports suggested that protein transduction is energy and temperature independent, these characteristics are now mostly attributed to phenomena such as fixation artefacts (Richard *et al.*, 2003). More recent data indicate that basic PTDs such as Tat enter the cells through a macropinocytotic pathway that is universally active in all cells (Wadia *et al.*, 2004; Kaplan *et al.*, 2005). A series of events involves Tat attachment to an anionic cell surface,

followed by the association of these complexes with lipid rafts, which triggers dynamin-independent macropinocytosis. After internalization, the endosome pH falls and Tat apparently destabilizes the membranes, which results in a small amount of the endosome contents escaping into the cytosol. The released fraction of Tat can then exert its biologic activity. Consistent with this model, Tat delivery is enhanced by the influenza virus haemagglutinin fusogenic motif, which further destabilizes endosomal membranes at a low pH (Han *et al.*, 2001; Skehel *et al.*, 2001). In cells cotreated with Tat-conjugated HA2 (HA2-Tat), a greater proportion of endocytosed Tat-fused Cre recombinase escapes into the cytoplasm (Wadia *et al.*, 2004). Other studies suggest that certain cell types might incorporate Tat constructs by clathrin- or caveolin-dependent endocytosis, raising the possibility that transport varies according to the cargo or cell type (Ferrari *et al.*, 2003; Fittipaldi *et al.*, 2003; Richard *et al.*, 2005). In addition to the basic Tat peptide, there are other proteins (fragments), such as antennapedia (Antp), Rev and VP22, that enhance cellular uptake of proteins (Table 1) (Derossi *et al.*, 1994; Elliott and O'Hare, 1997; Futaki *et al.*, 2001; Joliot and Prochiantz, 2004). These four well-known PTDs facilitate the delivery of various biomacromolecules into the cell, but few studies have examined their relative efficacy.

In the present study, we evaluated the potency and internalizing pathway of four major PTDs to optimize protein transduction technology and to clarify the mechanisms of action. We also evaluated the cytotoxicity of these four PTDs as this is crucial to their utility as effective biomacromolecule carriers. These analyses may help not only to elucidate the mechanism by which the four peptides facilitate the cellular uptake of biomacromolecules, but also provide criteria for their proper use.

Materials and methods

Cell lines

HeLa cells (human cervical carcinoma cells) and A431 cells (human epithelial carcinoma cells) were obtained from the American Type Culture Collection (Manassas, VA, USA). HaCaT cells (human keratinocyte cells) were kindly provided by Dr S Inui, Osaka University. Jurkat cells (human leukaemia cells) and MOLT-4 cells (human leukaemia cells) were kindly provided by Hayashibara Biochemical Laboratories Inc. (Okayama, Japan). HL60 cells (human promyelocytic leukaemia cells) were obtained from the Japanese Collection of Research Bioresources (JCRB; Osaka, Japan). HeLa cells were cultured in minimal essential medium (MEMα; Wako Pure Chemicals, Osaka, Japan) medium supplemented with 10% fetal bovine serum (FBS) and antibiotics. A431 cells and HaCaT cells were maintained in Dulbecco's modified Eagle's medium (Wako Pure Chemicals) supplemented with 10% FBS, 1% L-glutamine and antibiotics. Jurkat cells and MOLT-4 cells were maintained in RPMI-1640 medium (Wako Pure Chemicals) supplemented with 10% FBS and antibiotics. HL60 cells were maintained in RPMI-1640 medium (Wako Pure Chemicals) supplemented with 20% FBS and antibiotics. All cells were cultured at 37 C in 5% CO_2.

Table 1 Protein sequences of the PTDs evaluated

PTD	*Origin*	*Sequence*	*pI*
Tat	HIV-1	G**RKKRR**Q**RRR**PPQ	12.70
Antp	*Drosophila*	**RQIKIWFQNRRMKWKK**	12.31
Rev	HIV-1	T**RQARRNRRRR**W**RERQ**F	12.60
VP22	HSV	NAKT**RRHERRRK**LAIER	12.01

The basic amino acids in each sequence are shown in bold.

Synthetic peptides

All peptides used in this study were purchased from the Toray Research Center Inc. (Tokyo, Japan) and had purities above 90%, which was confirmed by high-performance liquid chromatography analysis and mass spectroscopy. The sequences of these peptides were GRKKRRQRRRPPQK-FAM (FAM = carboxyfluorescein) for Tat-conjugated FAM (Tat-FAM), RQIKIWFQNRRMKWKKK-FAM for Antp-conjugated FAM (Antp-FAM), TRQARRNRRRRWRERQRK-FAM for Rev-conjugated FAM (Rev-FAM), NAKTRRHERRRKLAIERK-FAM for VP22-conjugated FAM (VP22-FAM), YGRKKRRQRRRK-biotin for Tat-conjugated biotin, RQIKIWFQNRRMKWKKK-biotin Antp-conjugated biotin, TQRARRNRRRRWRERQRK-biotin for Rev-conjugated biotin, NAKTRRHERRRKLAIERK-biotin for VP22-conjugated biotin and GLFEAIEGFIENGWEGMIDGWY GYGRKKRRQRRR for HA2-conjugated Tat (HA2-Tat). The individual PTD sequences are underlined.

Flow cytometric analysis

HeLa cells, HaCaT cells and A431 cells were cultured in 24-well plates (Nalge Nunc International, Naperville, IL, USA) at 5.0×10^4 cells per well in culture medium and incubated for 24 h at 37 C. Jurkat cells, MOLT-4 cells and HL60 cells were cultured in 24-well plates (Nalge Nunc International) at 1.0×10^5 cells per well in Opti-MEM I (Invitrogen, Carlsbad, CA, USA). After aspirating the media, FAM-conjugated PTD (PTD-FAM) (10 μM) was added to the cells in Opti-MEM I and the culture dishes were incubated for an additional 3 h. Following incubation, the cells were washed with phosphate-buffered saline and incubated for 5 min with 0.1% trypsin to detach them and to remove surface-bound peptides. After incubation, 2 vol of 10% FBS-containing culture medium was added to stop the trypsin activity and to detach the cells completely. The cell suspension was centrifuged at 800 *g*, washed with phosphate-buffered saline, centrifuged again and resuspended in 500 μl of 0.4% paraformaldehyde. Fluorescence was analysed on a FACSCalibur flow cytometer, and data were analysed using CellQuest software (both from Becton Dickinson, San Jose, CA, USA). In the low-temperature uptake experiment, cells were preincubated at 4 C for 1 h in Opti-MEM I prior to adding the PTDs, and all buffers and solutions were equilibrated to 4 C. To analyse the internalization mechanism, HeLa cells were pretreated for 30 min in Opti-MEM I medium with 0–5 mM methyl-β-cyclodextrin, 0–2.5 μM

cytochalasin D or 0–5 mM amiloride (all from Sigma-Aldrich, St Louis, MO, USA). After the PTD-FAMs were added, cells were maintained for 1 h (30 min for amiloride) in the presence of inhibitors and washed several times with phosphate-buffered saline. As a control, the cellular uptake of transferrin fluorescein isothiocyanate (Invitrogen) was also monitored.

Cell proliferation assay

Cell viability was determined using a WST-8 assay kit (Nacalai Tesque, Kyoto, Japan) according to the manufacturer's instructions. The assay is based on the cleavage of the tetrazolium salt WST-8 to formazan by cellular mitochondrial dehydrogenase. HeLa cells were cultured in 96-well plates (Nalge Nunc International) at 5.0×10^3 cells per well in MEMα and incubated for 24 h at 37 °C. Jurkat cells were cultured in 96-well plates at 1.0×10^4 cells per well in Dulbecco's modified Eagle's medium. The cells were treated with various concentrations of PTD-biotin. After 24 h incubation, cell viability was measured using the WST-8 assay kit.

Membrane integrity assay

The lactate dehydrogenase (LDH) leakage assay was used to quantify the membrane integrity of the PTD-treated cells. This assay detects the amount of LDH released into the culture media as a result of plasma membrane disruption after PTD treatment. HeLa cells were cultured in 96-well plates (Nalge Nunc International) at 5.0×10^3 cells per well in MEMα and incubated for 24 h at 37 °C. Jurkat cells were cultured in 96-well plates at 1.0×10^4 cells per well in Dulbecco's modified Eagle's medium. Each cell type was treated with various concentrations of PTD-biotin. After 3 h incubation, the LDH release activity of the peptides was measured using an LDH cytotoxicity test (Wako) according to the manufacturer's instructions.

Expression and purification of PTD-fused Venus protein

The Venus (variant of yellow fluorescent protein) DNA sequence was kindly provided by Dr A Miyawaki (RIKEN Brain Science Institute). The Tat-Venus DNA sequence was amplified by PCR. At the 5′ end, the primer sequence 5′-TTTAAGAAGGAGATATACATATGGCTTACGGTCGTAAAAAA CGTCGCCAGCGTCGCCGTGGTGGCGGCGGTTCCCTCGA GCACCACCATCACCACCATGTGAGCAAGGGCGAGGAGC TGTTCAC-3′ introduced an *Nde* I site and Tat sequence and at the 3′ end, the primer sequence 5′-GCTTTGTTAGCAG CCGAATTCTTACTTGTACAGCTCGTCCATGCCGAGAGTGA TC-3′ introduced an *Eco* RI site. The PCR product was digested with *Nde* I and *Eco* RI and inserted into a protein expression plasmid. Other plasmids expressing Antp-, Rev- or VP22-Venus recombinant proteins were constructed by replacing the Tat-coding region in the Tat-Venus plasmid with the Antp, Rev or VP22 sequences using the *Nde* I and *Xho* I restriction sites. These sequences were obtained by annealing the following oligonucleotides with protruding single-strand DNA corresponding to the *Nde* I and *Xho* I sites: Antp sense, 5′-TATGGCTCGTCAGATCAAAATCTGGTTCCA GAATCGTCGTATGAAGTGGAAAAAAGGTGGCGGCGGTTC CC-3′; Antp antisense, 5′-TCGAGGGAACCGCCGCCACCTT TTTTCCACTTCATACGACGATTCTGGAACCAGATTTTGATC TGACGAGCCA-3′; Rev sense, 5′-TATGGCTACCCGTCAGGC TCGTCGTAATCGTCGTCGTCGTTGGCGTGAACGTCAGCGT GGTGGCGGCGGTTCCC-3′; Rev antisense, 5′-TCGAGGGAA CCGCCGCCACCACGCTGACGTTCACGCCAACGACGACGA CGATTACGACGAGCCTGACGGGTAGCCA-3′; VP22 sense, 5′-TATGGCTAACGCTAAAACCCGTCGTCACGAACGTCGTCG TAAACTGGCTATCGAACGTGGTGGCGGCGGTTCCC-3′; VP22 antisense, 5′-TCGAGGGAACCGCCGCCACCACGTTCGATAG CCAGTTTACGACGACGTTCGTGACGACGGGTTTTAGCGT TAGCCA-3′. The plasmids, except for the Antp-Venus expression vector, were transformed into *Escherichia coli* BL21 Star (DE3) (Invitrogen). The Antp-Venus-expressing vector was transformed into BL21 Star (DE3), in which the plasmid-expressing chaperone (pGro7) was pretransformed. Transformed *E. coli* was cultured and the cell paste was suspended in BugBuster Master Mix (Novagen, Darmstadt, Germany) and centrifuged. PTD-Venus was recovered in the supernatant and purified by His-tag affinity purification and gel filtration chromatography.

Confocal laser scanning microscopy analysis

HeLa cells were cultured on Lab-Tek II Chambered Coverglass (Nalge Nunc International) at 3.0×10^4 cells per well in MEMα supplemented with 10% FBS and incubated for 24 h at 37 °C. Internalization of PTD-FAM or PTD-Venus was performed as follows: HeLa cells were treated with PTD-FAM or PTD-Venus (10 μM) in Opti-MEM I containing 100 ng ml^{-1} Hoechst 33342 (Invitrogen) and 6 μg ml^{-1} FM4-64 (Invitrogen). After incubation at 37 °C for 3 h, the medium was exchanged with fresh medium and fluorescence was observed by confocal laser scanning microscopy (Leica Microsystems GmbH, Wetzlar, Germany) without cell fixation. For cotreatment with HA2-Tat, HeLa cells were cotreated with PTD-FAM (10 μM) and HA2-Tat (2 μM) in Opti MEM I containing 100 ng ml^{-1} Hoechst 33342. After incubation at 37 °C for 3 h, the medium was exchanged with fresh medium and fluorescence was observed by confocal laser scanning microscopy without cell fixation.

Results

Comparison of transduction efficiency and cytotoxicity of four PTDs

To confirm the intracellular translocation activity of the four selected PTDs, we evaluated the transduction efficiency of Tat-, Antp-, Rev- and VP22-FAM in six cell lines (adherent: HeLa, HaCaT and A431 cells; nonadherent: Jurkat, MOLT-4 and HL60 cells) using flow cytometric analysis (Figure 1). These PTDs contain a large number of basic amino acids (Table 1) and their cationic properties are thought to be important for cell membrane penetration (Futaki *et al.*, 2001; Chauhan *et al.*, 2007). Their positive charge, however, causes them to adsorb nonspecifically to negatively charged cell

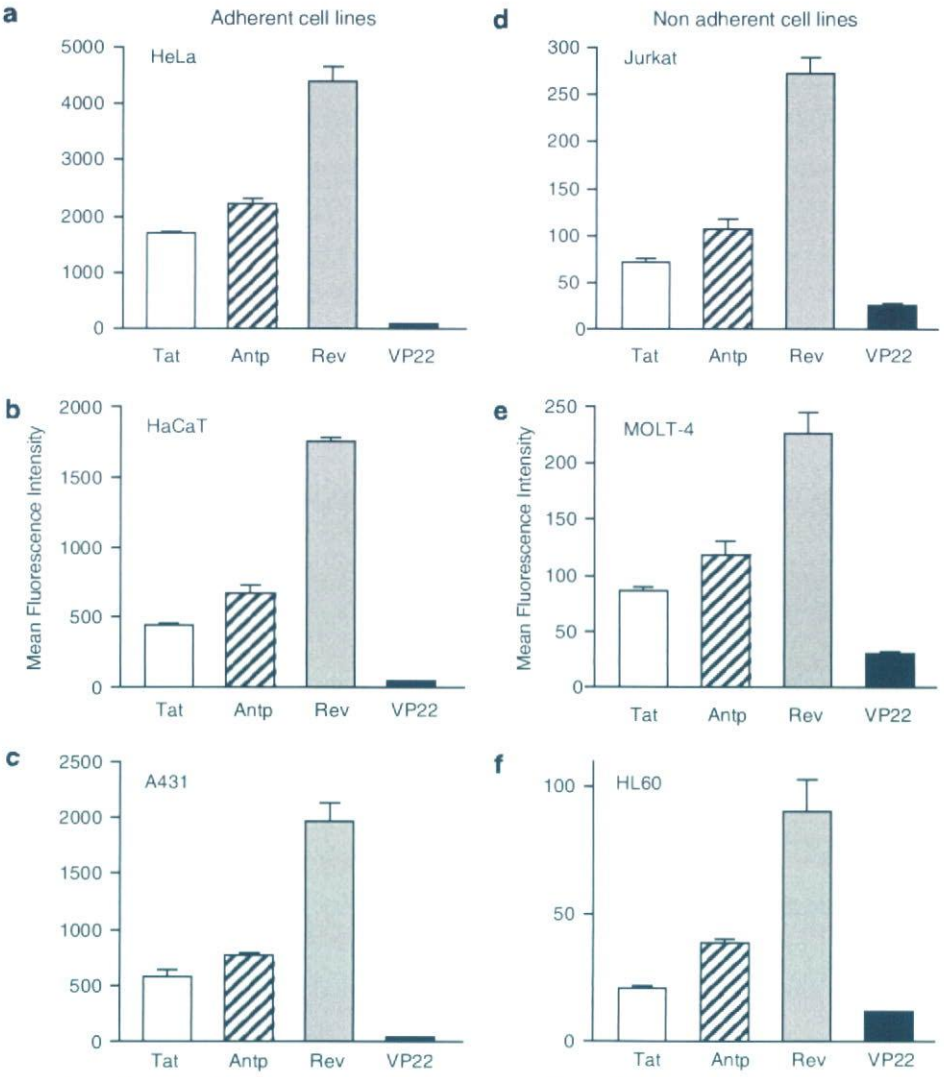

Figure 1 Comparison of the cellular uptake of protein transduction domains (PTDs). FAM-labelled Tat (white column), antennapedia (Antp; hatched column), Rev (grey column) and VP22 (black column) were incubated with six cell lines: HeLa (**a**), HaCaT (**b**), A431 (**c**), Jurkat (**d**), MOLT-4 (**e**) and HL60 (**f**) at 10 μM for 3 h. After trypsin treatment to digest PTDs adsorbed on the cell surface, the PTD-transduced cells were harvested and analysed by flow cytometry. Note that the *y* axis scales for the adherent cell lines are markedly different from that for the nonadherent cell lines. Data shown are the mean ± s.d. of triplicate assays.

membranes (Richard *et al.*, 2003). For this reason, the cells were treated with excess trypsin to eliminate nonspecific plasma membrane binding of the PTDs prior to measurement.

The relative order of their translocation efficiency (Rev > Antp > Tat > VP22), which was based on mean fluorescence, was independent of the cell type (that is, adherent or nonadherent). Furthermore, using PTD-fused Venus, we confirmed that Rev had the highest transduction efficiency (data not shown). Equally important, the overall translocation efficiency of the PTDs depended markedly on whether the cells were adherent (HeLa, HaCaT and A431 cells) or nonadherent (Jurkat, MOLT-4 and HL60 cells). The transduction efficiency was much higher in the adherent cell lines compared with the nonadherent cell lines (Figure 1); note that that the fluorescence (uptake) was about 8- to 25-fold greater in the adherent, than in nonadherent, cell lines.

The cytotoxic properties of the four PTDs were evaluated in adherent (HeLa) and nonadherent (Jurkat) cells. To assess the long-term changes in proliferation, mitochondrial dehydrogenase activity was measured using a WST-8 assay 24 h after PTD treatment. In HeLa cells, there was a remarkable decrease in cell viability when the cells were incubated with Antp at 100 μM, whereas other PTDs were not cytotoxic at the higher concentrations (Figure 2a). In contrast in Jurkat cells, Antp was extremely cytotoxic in a dose-dependent manner and Rev reduced cell proliferation by approximately 40% (Figure 2b). Previous reports indicated that amphipathic peptides, such as transportan, induced cytotoxicity by perturbing the cellular membrane (Hallbrink *et al.*, 2001; Jones *et al.*, 2005; Saar *et al.*, 2005; El-Andaloussi *et al.*, 2007). Thus, the membrane integrity of PTD-treated cells was also measured using an LDH leakage assay. Antp

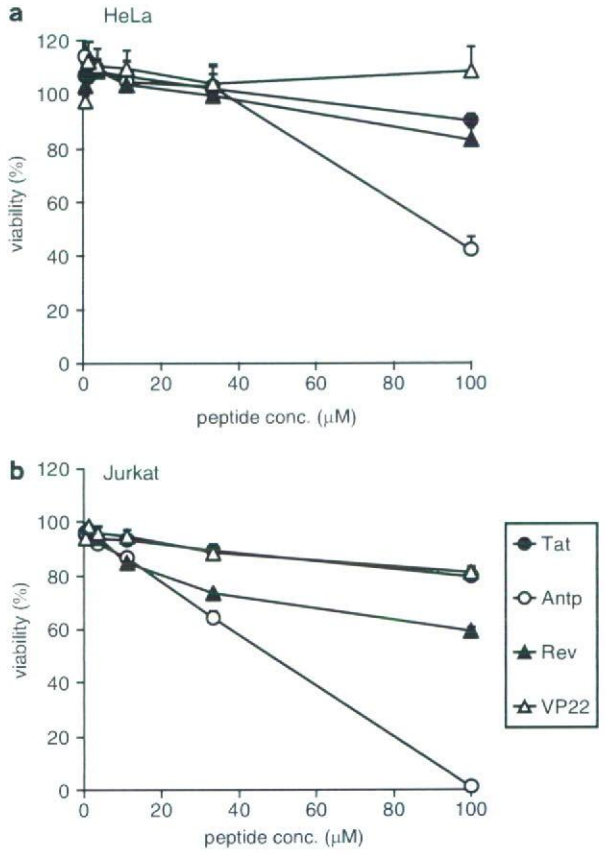

Figure 2 Viability of protein transduction domain (PTD)-treated cells. HeLa cells (**a**) and Jurkat cells (**b**) were incubated with serially diluted biotin-conjugated Tat, antennapedia (Antp), Rev and VP22 at 37 °C. After 24 h, cell viability was analysed using a WST-8 assay. Data shown are the mean ± s.d. of triplicate assays.

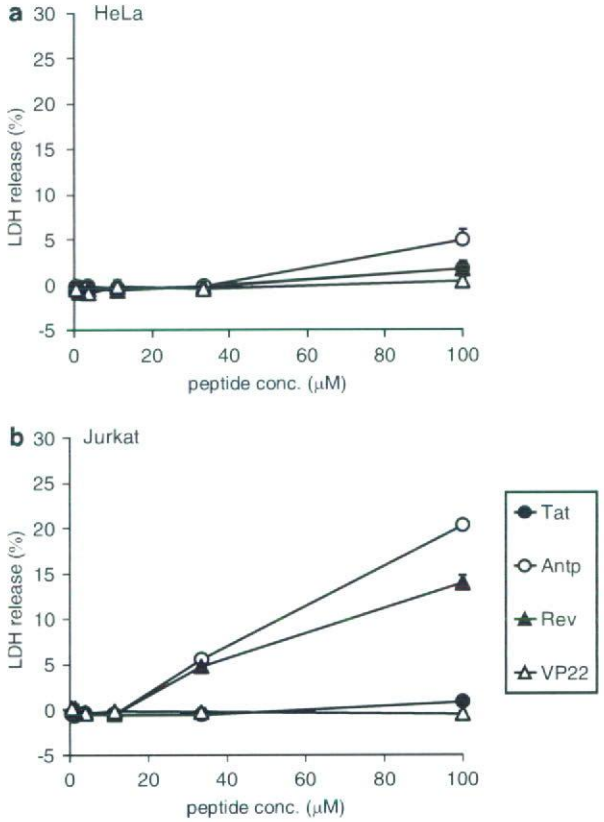

Figure 3 Membrane integrity of protein transduction domain (PTD)-treated cells. HeLa cells (**a**) and Jurkat cells (**b**) were incubated with serially diluted biotin-conjugated Tat, antennapedia (Antp), Rev and VP22 at 37 °C. After 3 h, the release of lactate dehydrogenase (LDH) was analysed. Data shown are the mean ± s.d. of triplicate assays.

and Rev induced significant LDH leakage in Jurkat cells, but only low LDH leakage was detected in Antp-treated HeLa cells (Figure 3). The membrane-perturbing effect of Antp and Rev contributed to the uptake of peptides, which are shown in Figure 1. Jurkat cells appear more sensitive to Antp or Rev treatment than HeLa cells; this difference in cytotoxicity and translocation efficiency may indicate a difference in the PTD-uptake mode.

Intracellular transduction mechanism of PTDs

The results of *in vitro* studies suggest that PTDs enter the cell via an energy-dependent endocytotic pathway (Lundberg *et al.*, 2003; Richard *et al.*, 2003). In particular, studies using various macropinocytosis inhibitors, such as methyl-β-cyclodextrin, to deplete cholesterol from the membrane (Grimmer *et al.*, 2002; Liu *et al.*, 2002), cytochalasin D, to inhibit F-actin elongation (Sampath and Pollard, 1991), or amiloride, to inhibit the Na^+-H^+ exchanger (West *et al.*, 1989), indicate that Tat is taken up into the cell via lipid raft-dependent macropinocytosis. To the best of our knowledge, however, few comparative studies have analysed the cellular uptake pathway of the four PTDs discussed in this paper. Therefore, we used flow cytometry analysis to determine whether PTD uptake is energy dependent or occurs via lipid raft-mediated macropinocytosis. First, we treated cells with PTD-FAM at 37 or 4 °C and then measured cell fluorescence (Figure 4). At 4 °C, transferrin, which enters cells by clathrin-dependent endocytosis (Schmid, 1997), inhibited the transduction efficiency compared with that at 37 °C. All four PTDs had low transduction ability at 4 °C, indicating that their cellular uptake was energy dependent. We next examined the PTD-FAM uptake efficiency in methyl-β-cyclodextrin-, cytochalasin D- and amiloride-treated HeLa cells. These cell treatments inhibited PTD-FAM incorporation in a dose-dependent manner, but transferrin was not affected (Figure 5). Furthermore, in HeLa cells treated with PTD-FAM, only punctuate fluorescence was observed using confocal laser scanning microscopic analysis (Figure 6). These results indicated that all the PTDs evaluated in this study enter the cell through the macropinocytotic pathway and that most of them were trapped in intracellular vesicles, the macropinosomes.

Intracellular localization of PTD–protein conjugates

We next examined the intracellular behaviour of the individual PTDs in more detail. To investigate whether

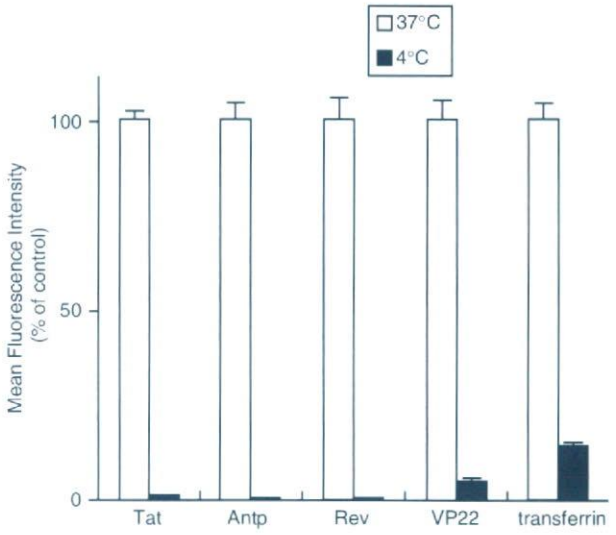

Figure 4 Effects of temperature on protein transduction domain (PTD) transduction efficiency. HeLa cells were preincubated at 37 or 4 °C for 1 h prior to adding FAM-labelled PTDs or fluorescein isothiocyanate-labelled transferrin for 3 h. Cells were washed in trypsin and analysed by flow cytometry. Data shown are the mean ± s.d. of triplicate assays.

individual PTDs are located in the same vesicles, we used Tat-fused HA2 peptide (HA2-Tat), an influenza virus-derived endosome-disrupting peptide. HA2-Tat improves the activity of Tat-fused Cre recombinase (Wadia *et al.*, 2004). Because HA2 alone cannot enter the cell, HA2-Tat is thought to enter the cell in a Tat-dependent manner and to disrupt the membrane of endosomal vesicles in which the Tat cargo is trapped. Thus, if Antp, Rev and VP22 are trapped in the same vesicles as Tat, the fluorescence should spread throughout the cytosol following cotreatment of the cells with HA2-Tat. As predicted, in HeLa cells cotreated with Antp-, Rev- or VP22-Venus and HA2-Tat, the Venus-derived fluorescence spread throughout the cytosol, whereas in the cells treated with Antp-, Rev- or VP22-Venus alone, only punctuate fluorescence was observed (Figure 7). These results suggested that all the PTDs evaluated in this study entered the cell through a macropinocytotic pathway and were trapped in the same vesicles as Tat.

Discussion

In the present study, we have systematically compared PTD-mediated molecular transduction mechanisms. Our findings indicated that individual PTDs have different levels of transduction efficiency and cytotoxicity, suggesting that PTDs are internalized into live cells via different mechanisms. We also examined the internalization pathway and intracellular localization of Tat, Antp, Rev and VP22. Unexpectedly, all the PTDs evaluated in this study entered the cell through the macropinocytotic pathway and were trapped in the same vesicles as Tat. The finding that the intracellular transduction pathways of the four PTDs were the same suggests that the method of cell internalization does not contribute to the

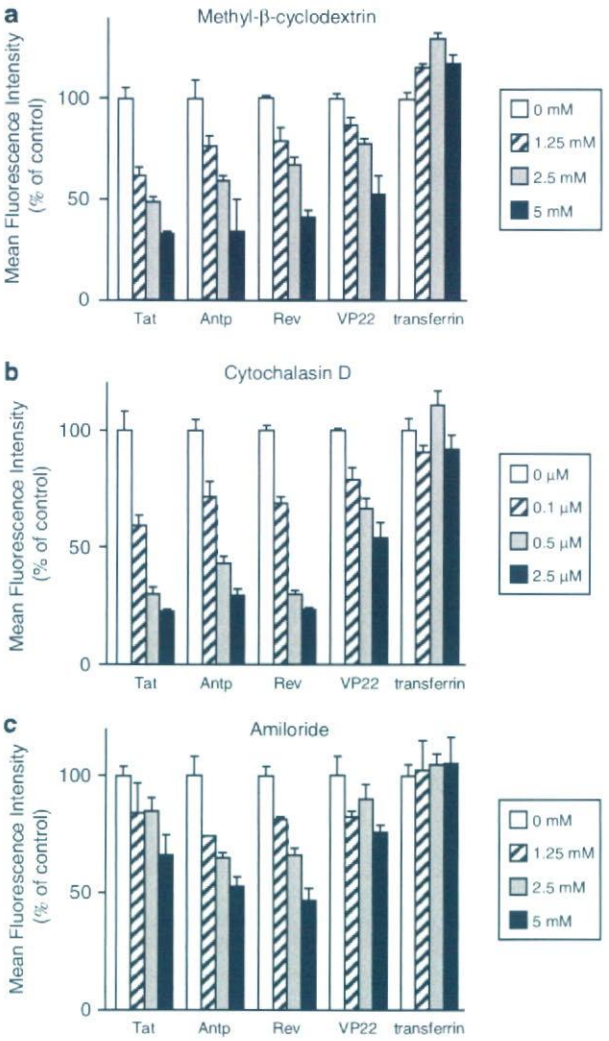

Figure 5 Effects of endocytosis inhibitors on transduction efficiency of protein transduction domains (PTDs). HeLa cells were pretreated with a range of concentrations of (**a**) methyl-β-cyclodextrin, (**b**) cytochalasin D or (**c**) amiloride for 30 min prior to adding FAM-labelled PTDs or fluorescein isothiocyanate-labelled transferrin for 1 h (**a** and **b**) or 30 min (**c**). Cells were washed in trypsin and analysed by flow cytometry. Data shown are the mean ± s.d. of triplicate assays.

differences in the PTD transduction efficiency or cytotoxicity. Although the reason for this phenomenon is not clear, we speculate that the primary structure of the individual PTDs or the cell surface proteins that interact with the individual PTDs contribute to the differences in their transduction efficiency and cytotoxicity.

The initial step in the mechanism of cellular entry of PTDs is thought to be the strong ionic interaction between the amino-acid residues of the PTDs and the plasma membrane constituents. Because the translocation is solely physically mediated, the charge distribution and amphipathicity of the peptide and its interaction with the plasma membrane is critical (Pujals *et al.*, 2006). Although most PTDs, if not all, contain a large number of basic amino acids, such as arginine or lysine, the theoretical isoelectric point (pI) value of each PTD used in this study was essentially identical (Tat, Antp,

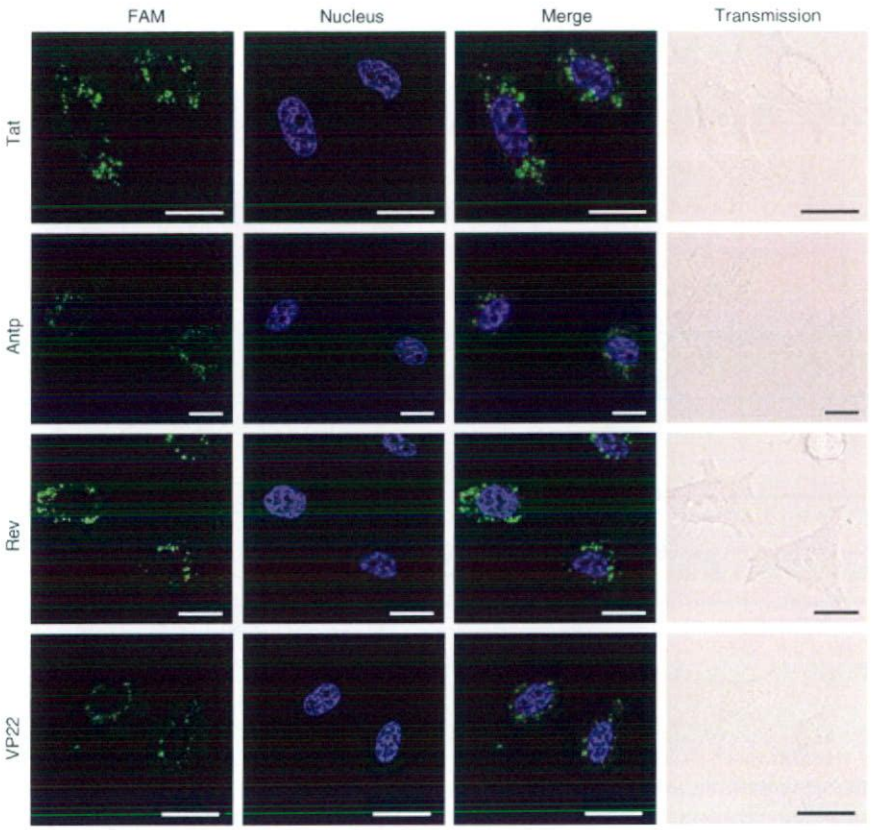

Figure 6 Intracellular behaviour of protein transduction domain (PTD)-FAM in living cells. HeLa cells were treated with 10 μM PTD-FAM for 3 h. Fluorescence images were acquired using confocal laser scanning microscopy and the signals were merged electronically. The nucleus was counterstained with Hoechst 33342 (blue). From top to bottom: Tat-, antennapedia (Antp)-, Rev- and VP22-FAM. From left to right: FAM (green), nucleus (blue), merged fluorescence and transmission image. Scale bars in each microphotograph indicate 20 μm.

Rev and VP22 have pI values of 12.70, 12.31, 12.60 and 12.01, respectively). Therefore, the internalization efficiency does not appear to depend on the cationic features of the PTDs.

The amphipathicity of the carrier is probably responsible not only for the strong interaction with the lipid membranes (Yandek *et al.*, 2007), but also for the disruption of the cellular membrane, which results in cell death (Hallbrink *et al.*, 2001; Jones *et al.*, 2005; Saar *et al.*, 2005; El-Andaloussi *et al.*, 2007). In terms of cytotoxicity, our data indicate that Antp and Rev both disrupt the membrane (Figure 3), but Rev does not contain an amphipathic structure. Furthermore, there was no correlation between hydrophobicity and transduction efficiency. Thus, differences in the PTD-mediated transduction efficiency and cytotoxicity might be due to the molecular weight or pI of the conjugated cargo.

The cellular events required for internalization, however, differ between reports and are often conflicting. The first mechanistic studies led to the proposal that PTD internalization occurs rapidly in a receptor- and energy-independent manner, perhaps by destabilizing the lipid bilayer or by the formation of inverted micelles with subsequent release of their contents within the intracellular space (Berlose *et al.*, 1996). More recently, an active mechanism based on vesicular uptake was proposed as the general mode of cell internalization of PTDs. In our experiment, although all four PTDs tended to be present in the same vesicles, the detailed mechanism for this colocalization is not yet known. It has been suggested that PTD internalization requires cell surface heparan sulphate proteoglycans (Tyagi *et al.*, 2001; Console *et al.*, 2003; Ziegler and Seelig, 2004). Because Tat interacts electrostatically with heparan sulphate proteoglycan present on the cell surface, it is possible that some PTDs are taken into the same vesicles when they interact with one heparan sulphate proteoglycan. In contrast, as shown in Figure 7, although fluorescence was observed throughout the cytosol, punctate fluorescence was also observed when the cells were cotreated with PTD-Venus and HA2-Tat. This finding suggested that the PTDs did not all exist in the same vesicles and that some PTDs entered the cell through another pathway. This is just speculation, however, and we are now using proteome analysis, such as liquid chromatography coupled with mass spectrometry or two-dimensional gel electrophoresis, to examine whether there are individual cell surface receptors for different PTDs.

In summary, our data suggest that Antp, Rev, VP22 and Tat cross the plasma membrane and reach the macropinosomes via different mechanisms. Our findings also indicate that several issues, such as endosome entrapment and low cell specificity, which limit the therapeutic activity of the cargo,

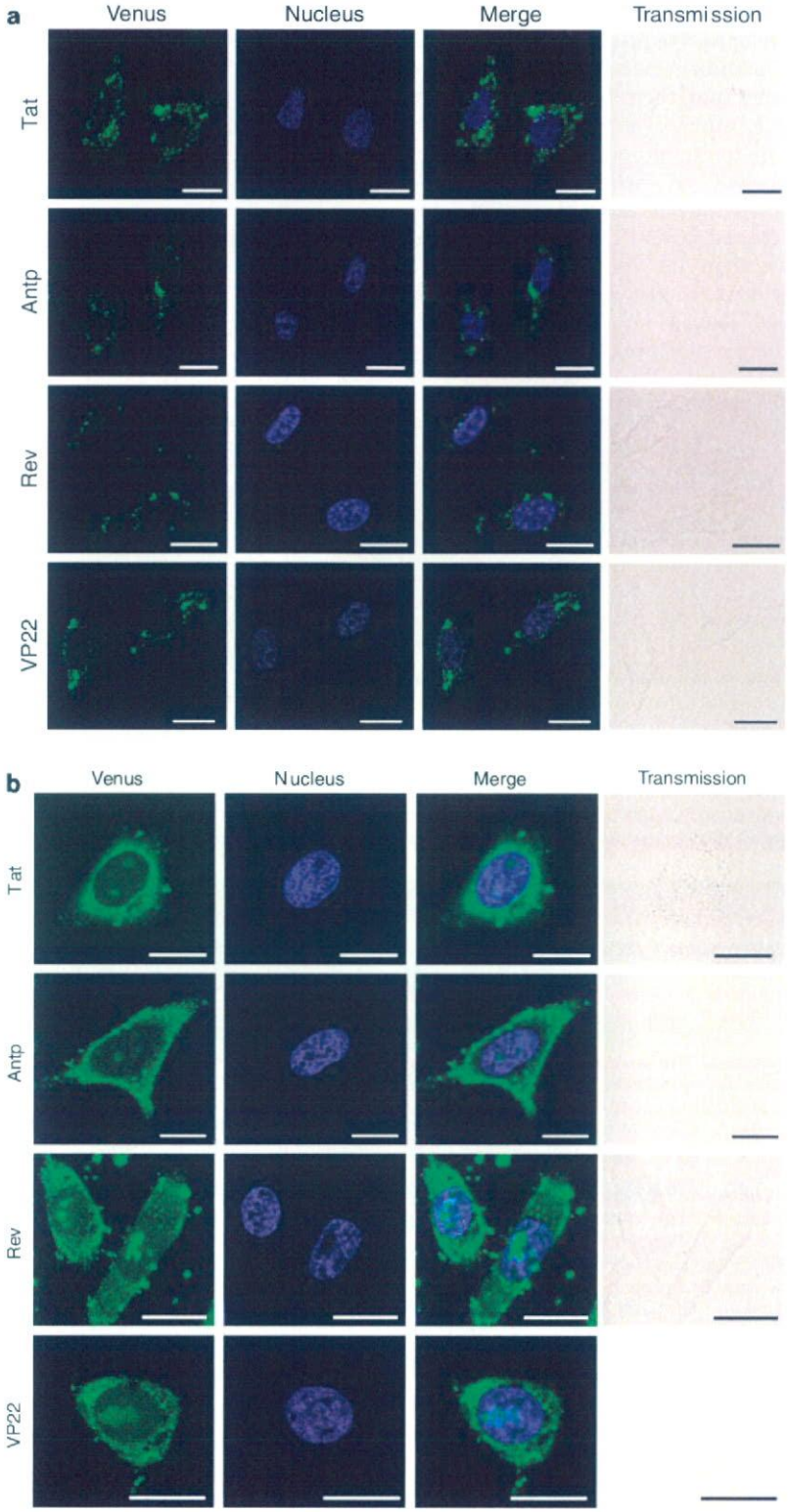

Figure 7 Intracellular behaviour of protein transduction domain (PTD)-Venus in living cells. HeLa cells were treated with 10 μM PTD-Venus alone (**a**) or 10 μM HA2-Tat (**b**) for 3 h. Fluorescence images were acquired using confocal laser scanning microscopy and the signals were merged electronically. The nucleus was counterstained with Hoechst 33342 (blue). From top to bottom: Tat-, antennapedia (Antp)-, Rev- and VP22-Venus. From left to right: Venus (green), nucleus (blue), merged fluorescence and transmission image. Scale bars in each microphotograph indicate 20 μm.

must be overcome before effective PTD-based drug delivery carriers can be fully developed. We previously reported that cotreatment with HA2-Tat enhances the cytosolic release of Tat-fused peptide-blockers and their biological activities, thereby overcoming the issue of endosome entrapment (Sugita *et al.*, 2007). Furthermore, although the transduction mechanism of PTDs is not yet well understood, these differences led us to explore the possibility of creating novel PTDs. We successfully created novel PTDs that have higher transduction efficiencies than Tat, using a unique phage display-based screening strategy that we previously developed (Mukai *et al.*, 2006; Kamada *et al.*, 2007). Moreover, based on our PTD-screening system, we are currently working to create more useful PTDs with cell type specificity.

Conflict of interest

The authors state no conflict of interest.

References

Berlose JP, Convert O, Derossi D, Brunissen A, Chassaing G (1996). Conformational and associative behaviours of the third helix of antennapedia homeodomain in membrane-mimetic environments. *Eur J Biochem* **242**: 372–386.

Borsello T, Forloni G (2007). JNK signalling: a possible target to prevent neurodegeneration. *Curr Pharm Des* **13**: 1875–1886.

Brusic V, Marina O, Wu CJ, Reinherz EL (2007). Proteome informatics for cancer research: from molecules to clinic. *Proteomics* **7**: 976–991.

Chauhan A, Tikoo A, Kapur AK, Singh M (2007). The taming of the cell penetrating domain of the HIV Tat: myths and realities. *J Control Release* **117**: 148–162.

Console S, Marty C, Garcia-Echeverria C, Schwendener R, Ballmer-Hofer K (2003). Antennapedia and HIV transactivator of transcription (TAT) 'protein transduction domains' promote endocytosis of high molecular weight cargo upon binding to cell surface glycosaminoglycans. *J Biol Chem* **278**: 35109–35114.

Derossi D, Joliot AH, Chassaing G, Prochiantz A (1994). The third helix of the Antennapedia homeodomain translocates through biological membranes. *J Biol Chem* **269**: 10444–10450.

Drabik A, Bierczynska-Krzysik A, Bodzon-Kulakowska A, Suder P, Kotlinska J, Silberring J (2007). Proteomics in neurosciences. *Mass Spectrom Rev* **26**: 432–450.

El-Andaloussi S, Jarver P, Johansson HJ, Langel U (2007). Cargo dependent cytotoxicity and delivery efficacy of cell-penetrating peptides: a comparative study. *Biochem J* **407**: 285–292.

Elliott G, O'Hare P (1997). Intercellular trafficking and protein delivery by a herpesvirus structural protein. *Cell* **88**: 223–233.

Ferrari A, Pellegrini V, Arcangeli C, Fittipaldi A, Giacca M, Beltram F (2003). Caveolae-mediated internalization of extracellular HIV-1 tat fusion proteins visualized in real time. *Mol Ther* **8**: 284–294.

Fittipaldi A, Ferrari A, Zoppe M, Arcangeli C, Pellegrini V, Beltram F *et al.* (2003). Cell membrane lipid rafts mediate caveolar endocytosis of HIV-1 Tat fusion proteins. *J Biol Chem* **278**: 34141–34149.

Futaki S, Suzuki T, Ohashi W, Yagami T, Tanaka S, Ueda K *et al.* (2001). Arginine-rich peptides. An abundant source of membrane-permeable peptides having potential as carriers for intracellular protein delivery. *J Biol Chem* **276**: 5836–5840.

Grimmer S, van Deurs B, Sandvig K (2002). Membrane ruffling and macropinocytosis in A431 cells require cholesterol. *J Cell Sci* **115**: 2953–2962.

Hallbrink M, Floren A, Elmquist A, Pooga M, Bartfai T, Langel U (2001). Cargo delivery kinetics of cell-penetrating peptides. *Biochim Biophys Acta* **1515**: 101–109.

Han X, Bushweller JH, Cafiso DS, Tamm LK (2001). Membrane structure and fusion-triggering conformational change of the fusion domain from influenza hemagglutinin. *Nat Struct Biol* **8**: 715–720.

Hawiger J (1999). Noninvasive intracellular delivery of functional peptides and proteins. *Curr Opin Chem Biol* **3**: 89–94.

Joliot A, Prochiantz A (2004). Transduction peptides: from technology to physiology. *Nat Cell Biol* **6**: 189–196.

Jones SW, Christison R, Bundell K, Voyce CJ, Brockbank SM, Newham P *et al.* (2005). Characterisation of cell-penetrating peptide-mediated peptide delivery. *Br J Pharmacol* **145**: 1093–1102.

Kamada H, Okamoto T, Kawamura M, Shibata H, Abe Y, Ohkawa A *et al.* (2007). Creation of novel cell-penetrating peptides for intracellular drug delivery using systematic phage display technology originated from Tat transduction domain. *Biol Pharm Bull* **30**: 218–223.

Kaplan IM, Wadia JS, Dowdy SF (2005). Cationic TAT peptide transduction domain enters cells by macropinocytosis. *J Control Release* **102**: 247–253.

Liu NQ, Lossinsky AS, Popik W, Li X, Gujuluva C, Kriederman B *et al.* (2002). Human immunodeficiency virus type 1 enters brain microvascular endothelia by macropinocytosis dependent on lipid rafts and the mitogen-activated protein kinase signaling pathway. *J Virol* **76**: 6689–6700.

Lundberg M, Wikstrom S, Johansson M (2003). Cell surface adherence and endocytosis of protein transduction domains. *Mol Ther* **8**: 143–150.

Mukai Y, Sugita T, Yamato T, Yamanada N, Shibata H, Imai S *et al.* (2006). Creation of novel protein transduction domain (PTD) mutants by a phage display-based high-throughput screening system. *Biol Pharm Bull* **29**: 1570–1574.

Murriel CL, Dowdy SF (2006). Influence of protein transduction domains on intracellular delivery of macromolecules. *Expert Opin Drug Deliv* **3**: 739–746.

Nagahara H, Vocero-Akbani AM, Snyder EL, Ho A, Latham DG, Lissy NA *et al.* (1998). Transduction of full-length TAT fusion proteins into mammalian cells: TAT-p27Kip1 induces cell migration. *Nat Med* **4**: 1449–1452.

Nori A, Kopecek J (2005). Intracellular targeting of polymer-bound drugs for cancer chemotherapy. *Adv Drug Deliv Rev* **57**: 609–636.

Pujals S, Fernandez-Carneado J, Lopez-Iglesias C, Kogan MJ, Giralt E (2006). Mechanistic aspects of CPP-mediated intracellular drug delivery: relevance of CPP self-assembly. *Biochim Biophys Acta* **1758**: 264–279.

Rhodes DR, Chinnaiyan AM (2005). Integrative analysis of the cancer transcriptome. *Nat Genet* **37** (Suppl): S31–S37.

Richard JP, Melikov K, Brooks H, Prevot P, Lebleu B, Chernomordik LV (2005). Cellular uptake of unconjugated TAT peptide involves clathrin-dependent endocytosis and heparan sulfate receptors. *J Biol Chem* **280**: 15300–15306.

Richard JP, Melikov K, Vives E, Ramos C, Verbeure B, Gait MJ *et al.* (2003). Cell-penetrating peptides. A reevaluation of the mechanism of cellular uptake. *J Biol Chem* **278**: 585–590.

Rojas M, Donahue JP, Tan Z, Lin YZ (1998). Genetic engineering of proteins with cell membrane permeability. *Nat Biotechnol* **16**: 370–375.

Saar K, Lindgren M, Hansen M, Eiriksdottir E, Jiang Y, Rosenthal-Aizman K *et al.* (2005). Cell-penetrating peptides: a comparative membrane toxicity study. *Anal Biochem* **345**: 55–65.

Sampath P, Pollard TD (1991). Effects of cytochalasin, phalloidin, and pH on the elongation of actin filaments. *Biochemistry* **30**: 1973–1980.

Schmid SL (1997). Clathrin-coated vesicle formation and protein sorting: an integrated process. *Annu Rev Biochem* **66**: 511–548.

Schwarze SR, Ho A, Vocero-Akbani A, Dowdy SF (1999). *In vivo* protein transduction: delivery of a biologically active protein into the mouse. *Science* **285**: 1569–1572.

Schwarze SR, Hruska KA, Dowdy SF (2000). Protein transduction: unrestricted delivery into all cells? *Trends Cell Biol* **10**: 290–295.

Skehel JJ, Cross K, Steinhauer D, Wiley DC (2001). Influenza fusion peptides. *Biochem Soc Trans* **29**: 623–626.

Sugita T, Yoshikawa T, Mukai Y, Yamanada N, Imai S, Nagano K *et al.* (2007). Improved cytosolic translocation and tumor-killing

activity of Tat-shepherdin conjugates mediated by co-treatment with Tat-fused endosome-disruptive HA2 peptide. *Biochem Biophys Res Commun* **363**: 1027–1032.

Tyagi M, Rusnati M, Presta M, Giacca M (2001). Internalization of HIV-1 tat requires cell surface heparan sulfate proteoglycans. *J Biol Chem* **276**: 3254–3261.

Wadia JS, Stan RV, Dowdy SF (2004). Transducible TAT-HA fusogenic peptide enhances escape of TAT-fusion proteins after lipid raft macropinocytosis. *Nat Med* **10**: 310–315.

West MA, Bretscher MS, Watts C (1989). Distinct endocytotic pathways in epidermal growth factor-stimulated human carcinoma A431 cells. *J Cell Biol* **109**: 2731–2739.

Yandek LE, Pokorny A, Floren A, Knoelke K, Langel U, Almeida PF (2007). Mechanism of the cell-penetrating peptide transportan 10 permeation of lipid bilayers. *Biophys J* **92**: 2434–2444.

Ziegler A, Seelig J (2004). Interaction of the protein transduction domain of HIV-1 TAT with heparan sulfate: binding mechanism and thermodynamic parameters. *Biophys J* **86**: 254–263.

Mini Review

Development of new anti-TNF therapy

Haruhiko Kamada *, Hiroko Shibata, and Yasuo Tsutsumi

Laboratory of Pharmaceutical Proteomics (LPP) National Institute of Biomedical Innovation (NIBIO), Osaka, Japan

We have generated the first TNFR1-selective antagonistic TNF mutant based on structural human TNF variants using our phage display technology. This TNF mutant did not activate TNFR1-mediated responses, although its affinity for TNFR1 was equivalent to human wild-type TNF (wtTNF). The TNF mutant neutralized wtTNF-induced TNFR1-mediated bioactivity without influencing TNFR2-mediated bioactivity. In hepatitis mouse models, the antagonistic TNF mutant significantly blocked liver injury caused by inflammation. These results indicate that antagonistic TNF mutants may be clinically useful for anti-TNF therapy and that phage display libraries of protein ligands can be used to select for receptor subtype-selective antagonists.

Rec.1/25/2007, Acc.4/16/2007, pp512-515

*Correspondence should be addressed to:
Haruhiko Kamada, Laboratory of Pharmaceutical Proteomics (LPP) National Institute of Biomedical Innovation (NIBIO) 7-6-8 Saito-Asagi, Ibaraki 567-0085, Osaka, Japan. Phone : +81-72-641-9811, FAX: +81-72-641-9817, e-mail: kamada@nibio.go.jp

Key words tumor necrosis factor-α, phage display system, protein mutant, TNF receptor specific antagonist, anti-TNF therapy

Inflammation is induced by physiological and chemical stimulation and is known to be mediated by the association of many biological factors. Inflammation-mediating proteins, typified by cytokines and chemokines, act in the host defense system by stimulating lymphocytes, macrophages, and endothelial cells to heal external injuries[1]. When a productive balance of these mediators collapses, inflammatory exacerbation occurs. Long-term over-expression of cytokines causes autoimmune disease[2]. Thus, development of therapeutic techniques to remedy the imbalance of cytokine production is necessary.

Tumor necrosis factor-α (TNF) is a major inflammatory cytokine and has a central role in host defense and inflammation[3]. To exert its biological function, TNF binds to two receptor subtypes, TNFR1 and TNFR2, which form homotrimers by preassembling on the cell surface[4]. Deregulation of TNF production promotes TNF-dependent pathologies and correlates with the severity and progression of inflammatory diseases such as rheumatoid arthritis (RA)[5], inflammatory bowel disease[6], septic shock[7] and hepatitis[8]. TNF blocking agents (monoclonal antibodies or soluble receptors) have shown significant clinical efficacy in certain inflammatory diseases. The major impact of TNF blocking agents on the immunological system, however, raises some concerns about the safety of this approach, especially with regard to severe infections[9], malignancies[10] and immune-mediated diseases[11]. For example, in rheumatoid arthritis and Crohn's disease, studies indicated a higher incidence of tuberculosis reactivation[12] and the induction of demyelination[13].

Although the distinction between the role of TNFR1 and TNFR2 on the immune system remains unclear, TNF secreted from activated immune cells in these diseases predominantly

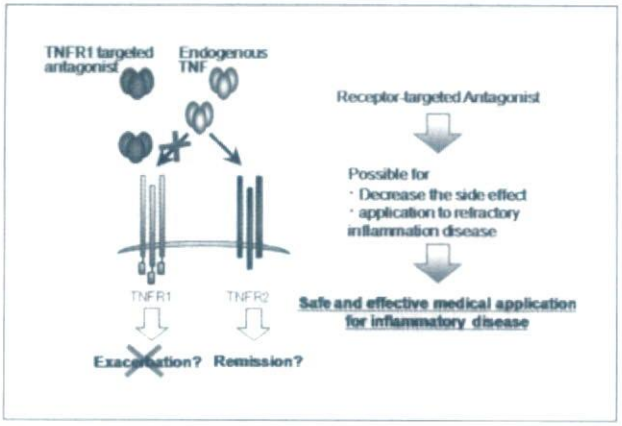

Fig.1 Generation antagonistic protein mutant for receptor targeting

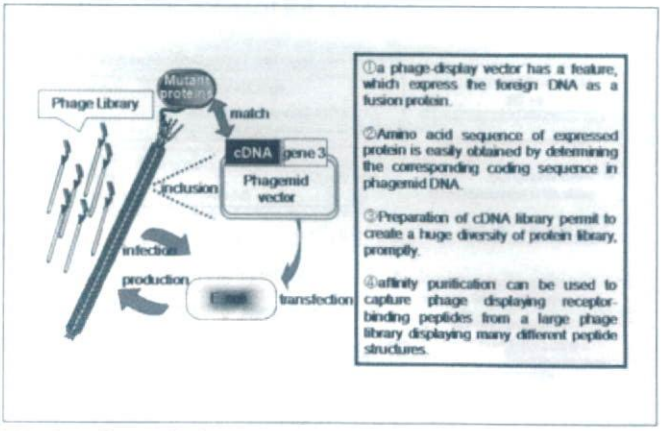

Fig.2 Benefit for engineering protein library using phage display system

activates TNFR1 and accelerates inflammation. In addition, previous studies using animal models of diseases such as arthritis[14] and hepatitis[15] indicated that mainly TNFR1 caused development and exacerbation of inflammation. Moreover, given that in mice lacking the TNFR1 the clinical course of EAE is suppressed both at the pro-inflammatory and the autoimmune phases, the TNFR1 is clearly indicated as an important target for therapy[16]. From this perspective, blocking TNFR1 signal transduction may emerge as a powerful and effective therapy for certain inflammatory diseases (Fig.1).

To develop receptor-selective protein ligands, several studies have described useful mutant proteins created by the substitution of amino acids using a site-directed mutagenesis method, as typified by Kunkel's method[17,18]. It is difficult, however, to obtain an exhaustive and functional panel of protein mutants using this mutagenesis method. Alternatively, the phage display system is a powerful *in vitro* technique that enables polypeptides with desired properties to be selected from a large collection of variants encoded by cDNAs in phagemid vectors (Fig.2). Filamentous phage display of peptide or protein variants has been widely used for rapid selection of protein variants that bind with improved affinity and specificity to target molecules[19]. The key feature of such selection schemes is that the genotype of a particular variant packaged inside a virion particle is linked to the phenotype of a displayed protein or peptide that has been fused to phage coat proteins, i.e., the gene III protein. Phage particles can be selected by binding to an affinity matrix propagated in E. coli and identified by DNA sequencing. These procedures allow phage libraries to be subjected to a selection step, called "affinity panning". Recovered clones are identified by sequencing and re-grown for further rounds of selection.

Using the phage display system, we previously isolated a lysine-deficient TNF mutant from a protein library in which all six lysine residues in the TNF molecule, including the receptor-binding site, were simultaneously replaced with other amino acids[19,20]. This strategy created novel mutant TNFs that exhibited only a slightly different mode of receptor-binding. In the present study, we used the phage display system to isolate novel TNFR1-selective antagonistic TNF mutants that efficiently inhibited a wide variety of TNFR1 mediated effects *in vitro* and *in vivo* without affecting TNFR2-mediated bioactivity.

The selection of amino acids to be altered was based on data from a point mutation study and a TNF structure-function study. Residues (amino acids 89-94) that were shown to contribute to TNFR binding were mapped onto the three-dimensional structure of human TNF. Then, these and other nearby residues were selected for randomization to generate phage libraries (Fig.3). Randomization of each of these residues was performed by PCR with mutated primers in which an NNS codon was incorporated at each randomized position. Each library contained a total of six randomized residues.

To select TNF mutants from phage library that bound strongly to human TNFR1, the mutant TNF phage library was panned against human TNFR1. As a result, we identified ten candidates as TNFR1-selective antagonists and selected the most suitable mutant that possessed the strongest antagonistic activity. To investigate the properties of this antagonistic clone, we examined the binding kinetics and binding specificities of this mutant for TNFR1 and TNFR2 using BIAcore and ELISA techniques, respectively. The antagonistic TNF mutant had an affinity for

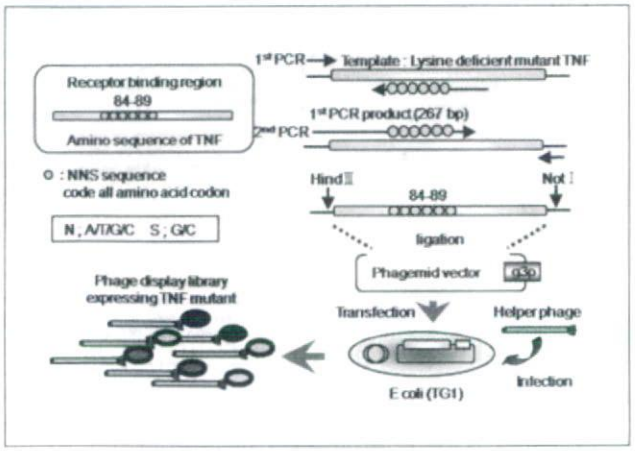

Fig.3 Engineering TNF mutant phage display library

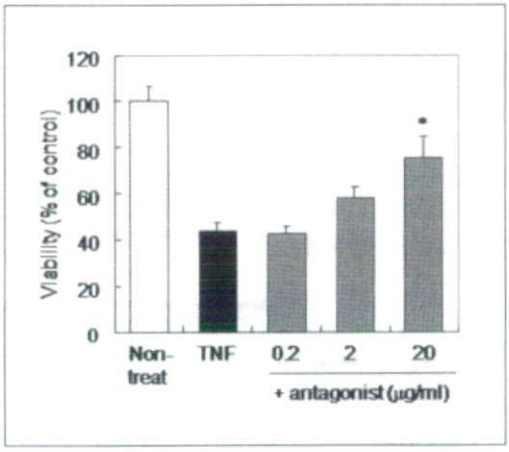

Fig.4 Inhibitory effect of antagonistic mutant TNF on TNF-induced cytotoxicity

Mouse fibrosarcoma L-M cells were treated with wild-type TNF (10 ng/ml). and serial diluted mutant TNF. After 48 hr incubation, ratio of cell death were determined by methylene blue assay.

TNFR1 equivalent to wtTNF, but almost no affinity for TNFR2. We also measured the bioactivity of the TNF mutant via TNFR-mediating response assays. The antagonistic TNF mutant bound to TNFR1 but did not transmit the death signal. To determine the ability of the TNF mutant to compete with wtTNF, we measured TNFR1-selective responses in the presence of both wtTNF and TNF mutant. The antagonistic TNF mutant inhibited wtTNF-induced cytotoxicity (Fig.4), caspase activation, and NF-κB activation through TNFR1 in a dose-dependent manner. These results suggest that the antagonistic TNF mutant is a competitive antagonist, inhibiting TNFR1-mediated pathways.

For the therapy of autoimmune disease, TNF blockades (etarnercept, as p75-IgG Fc fusion protein and lenercept as p55-IgG Fc fusion protein) have been developed. However, differences exist in the mechanisms of action of these agents that might confer risks of infection and immunogenisity. There are some reports that tuberculosis disease is a potential adverse reaction from treatment with etanercept. Moreover, antibody formation against lenercept was a significant problem which resulted in significant reduction of the half-life of the receptor. Thus, much is expected from the development of TNF receptor-selective agents that inhibit disease-causing TNF bioactivity without interfering host defense system against infection and antibody formation. In the present report, we generated a receptor-selective antagonistic TNF mutant through the use of phage display. However, there is a possibility of expressing the new function, which binds to another receptor like as TNF receptor superfamily. Therefore, the reasons of showing agonistic or antagonistic activity should be examined via structural analysis of binding sites. We are now analyzing the crystal structures of the complex formed between the antagonistic TNF mutant and TNFR1 so as to better understand the mechanisms of receptor subtype-selectivity.

While the functions of TNF and its receptors are unclear, their signaling specificities are being examined in many TNF-related studies. In this review, we studied mutant TNF antagonist that bound selectively to TNFR1. The findings from our TNFR1 and TNFR2 study are applicable to the receptors in the TNFR superfamily that do not contain a cytoplasmic death domain. However, we also have produced TNF agonist that binds to TNFR1 and TNFR2. These selective agonists and antagonists are not only therapeutically useful, but also are effective analytical tools for elucidating TNF receptor function. Further functional studies of TNF receptors could uncover interesting receptor biology and may yield additional targets for immunotherapy.

Acknowledgments

We thank Dr. Shinsaku Nakagawa and Dr. Rie Igarashi for publishing our work in this journal. This study was supported in part by Grants-in-Aid for Scientific Research (No.17689008, 17016084, 17790135, 18015055, 18659047) from the Ministry of Education, Culture, Sports, Science and Technology of Japan, in part by Health and Labor Sciences Research Grant from the Ministry of Health, Labor and Welfare of Japan, in part by Health Sciences Research Grants for Research on Health Sciences focusing on Drug Innovation from the Japan Health Sciences Foundation, in part by Takeda Science Foundation.

References

1) Tracey KJ, Cerami A: Tumor necrosis factor: a pleiotropic cytokine and therapeutic target. Annu Rev Med, 45: 491-503, 1994.
2) Cope AP: Regulation of autoimmunity by proinflammatory cytokines. Curr Opin Immunol, 10(6): 669-676, 1998.
3) Ware CF: Network communications: lymphotoxins, LIGHT, and TNF. Annu Rev Immunol, 23: 787-819, 2005.
4) Chan FK, Chun HJ, Zheng L, Siegel RM, Bui KL, Lenardo MJ: A domain in TNF receptors that mediates ligand-independent receptor assembly and signaling. Science, 288 (5475): 2351-2354, 2000.
5) Brennan FM, Feldmann M: Cytokines in autoimmunity. Curr Opin Immunol, 4(6): 754-759, 1992.
6) Van Deventer SJ: Tumour necrosis factor and Crohn's disease. Gut, 40(4): 443-448, 1997.
7) Dinarello CA, Gelfand JA, Wolff SM: Anticytokine strategies in the treatment of the systemic inflammatory response syndrome. Jama, 269(14): 1829-1835, 1993.
8) Bradham CA, Plumpe J, Manns MP, Brenner DA, Trautwein C: Mechanisms of hepatic toxicity. I.TNF-induced liver injury. Am J Physiol, 275(3 Pt 1): G387-G392, 1998.
9) Gardam MA, Keystone EC, Menzies R, Manners S, Skamene E, Long R, Vinh DC: Anti-tumour necrosis factor agents and tuberculosis risk: mechanisms of action and clinical management. Lancet Infect Dis, 3(3): 148-155, 2003.
10) Cohen RB, Dittrich KA: Anti-TNF therapy and malignancy--a critical review. Can J Gastroenterol, 15(6): 376-384, 2001.
11) Shakoor N, Michalska M, Harris CA, Block JA: Drug-induced systemic lupus erythematosus associated with etanercept therapy. Lancet, 359(9306): 579-580, 2002.
12) Keane J, Gershon S, Wise RP, Mirabile-Levens E, Kasznica J, Schwieterman WD, Siegel JN, Braun MM: Tuberculosis associated with infliximab, a tumor necrosis factor alpha-neutralizing agent. N Engl J Med, 345(15): 1098-1104, 2001.
13) Sicotte NL, Voskuhl RR: Onset of multiple sclerosis associated with anti-TNF therapy. Neurology, 57(10): 1885-1888, 2001.
14) Mori L, Iselin S, De Libero G, Lesslauer W: Attenuation of collagen-induced arthritis in 55-kDa TNF receptor type 1 (TNFR1)-IgG1-treated and TNFR1-deficient mice. J Immunol, 157(7): 3178-3182, 1996.
15) Tsuji H, Harada A, Mukaida N, Nakanuma Y, Bluethmann H, Kaneko S, Yamakawa K, Nakamura SI, Kobayashi KI, Matsushima K: Tumor necrosis factor receptor p55 is essential for intrahepatic granuloma formation and hepatocellular apoptosis in a murine model of bacterium-induced fulminant hepatitis. Infect Immun, 65(5): 1892-1898, 1997.
16) Kollias G, Kontoyiannis D: Role of TNF/TNFR in autoimmunity: specific TNF receptor blockade may be advantageous to anti-TNF treatments. Cytokine Growth Factor Rev, 13(4-5): 315-321, 2002.
17) Kunkel TA: Rapid and efficient site-specific mutagenesis without phenotypic selection. Proc Natl Acad Sci USA, 82 (2): 488-492, 1985.
18) Yamagishi J, Kawashima H, Matsuo N, Ohue M, Yamayoshi M, Fukui T, Kotani H, Furuta R, Nakano K, Yamada M: Mutational analysis of structure--activity relationships in human tumor necrosis factor-alpha. Protein Eng, 3(8): 713-719, 1990.
19) McCafferty J, Griffiths AD, Winter G, Chiswell DJ: Phage antibodies: filamentous phage displaying antibody variable domains. Nature, 348(6301): 552-554, 1990.
20) Shibata H, Yoshioka Y, Ikemizu S, Kobayashi K, Yamamoto Y, Mukai Y, Okamoto T, Taniai M, Kawamura M, Abe Y, Nakagawa S, Hayakawa T, Nagata S, Yamagata Y, Mayumi T, Kamada H, Tsutsumi Y: Functionalization of tumor necrosis factor-alpha using phage display technique and PEGylation improves its antitumor therapeutic window. Clin Cancer Res, 10(24): 8293-8300, 2004.

Hepatoprotective Effect of Vitamin B_{12} on Dimethylnitrosamine-Induced Liver Injury

Katsuhiro ISODA,[a] Noritaka KAGAYA,[a] Soichiro AKAMATSU,[a] Shinji HAYASHI,[a] Makoto TAMESADA,[b] Aiko WATANABE,[b] Masakazu KOBAYASHI,[b] Yoh-ichi TAGAWA,[c] Masuo KONDOH,[a] Masaya KAWASE,[d] and Kiyohito YAGI*,[a]

[a] *Graduate School of Pharmaceutical Sciences, Osaka University; 1–6 Yamada-oka, Suita, Osaka 565–0871, Japan:* [b] *Research and Development Center, Kobayashi Pharmaceutical Co., Ltd.; 1–30–3 Toyokawa, Ibaraki, Osaka 567–0057, Japan:* [c] *Department of Biomolecular Engineering, Graduate School of Bioscience and Biotechnology, Tokyo Institute of Technology; 4259 Nagatsuta-cho, Yokohama, Kanagawa 226–8501, Japan: and* [d] *Faculty of Pharmaceutical Sciences, Osaka-Ohtani University; 3–11–1 Nishikiori-kita, Tondabayashi, Osaka 584–8540, Japan.*

Received August 21, 2007; accepted November 9, 2007; published online November 19, 2007

Vitamin B_{12} contains a cobalt complex and accumulates at high levels in the liver. Vitamin B_{12} was examined for its hepatoprotective effect on dimethylnitrosamine-induced liver injury in mice. Vitamin B_{12} decreased the blood levels of aspartate aminotransferase and alanine aminotransferase, and clearly inhibited the overaccumulation of collagen fibrils. Reverse transcription-polymerase chain reaction (RT-PCR) analysis of the liver showed that the gene expression of α-smooth muscle actin and heat-shock protein 47, which are markers of fibrosis, were suppressed by vitamin B_{12} administration. Our findings indicate that vitamin B_{12} could be an effective hepatoprotective agent.

Key words hepatoprotection; vitamin B_{12}; liver fibrosis; metal complex

The incidence of hepatoma related to hepatitis C and B continues to increase in developed countries. Chronic liver injury, including that caused by virus infection, cause persistent inflammation and fibrosis, followed by the development of liver cirrhosis and hepatoma. The use of interferon (IFN) has become the first-line treatment for viral hepatitis, but it is not effective in patients with a high viral load. Recently, investigators have begun to seek hepatoprotective agents that might facilitate the treatment of liver failure.

Vitamin B_{12} contains a cobalt complex and is therefore also known as cobalamin.[1] Its molecular weight is the largest of all the vitamins, and it is known to accumulate at high levels in the liver. Therefore, the concentration of vitamin B_{12} in the blood rises in the presence of acute or chronic liver disease.[2,3] Also, vitamin B_{12} associates with many enzymes, such as adenosylcobalamin-dependent isomerases, methylcobalamin-dependent methyltransferases, and dehalogenases.[4] Chronic feeding of a methyl-donor, vitamin B_{12}-deficient diet causes the spontaneous development of hepatocellular carcinoma.[5] Therefore, when the liver is injured, stored vitamin B_{12} leaks out into the blood, which causes a severe B_{12}-deficit in the liver, probably resulting in metabolic dysfunction. So far, it has been reported that vitamin B_{12} was effective for the liver protection against the acute liver injury.[6] However, there is no findings of the effect on chronic liver fibrosis. Therefore, we examined the effect of vitamin B_{12} on the fibrogenesis using chronically liver-injured mice.

Dimethylnitrosamine (DMN) is a potent hepatotoxin, carcinogen and mutagen. DMN induces liver fibrosis in a highly reproducible manner, first inducing a central hemorrhagic necrosis followed by the formation of septa and establishing micronodular cirrhosis after 3 weeks of treatment.[7] DMN-induced liver fibrosis in animals is a good and reproducible animal model for studying pathophysiological alterations associated with the development of liver fibrosis and cirrhosis in humans.[8,9] In this study, we found that the treatment of a chronic liver-injury model with vitamin B_{12} suppressed both liver inflammation and fibrosis.

MATERIALS AND METHODS

Animals BALB/c mice were purchased from SLC (Shimizu, Japan). The animals were housed in an air-conditioned room at 22 °C before the experiment. Hepatic injury in mice aged 6 weeks was elicited by the intraperitoneal administration of dimethylnitrosamine (DMN; Sigma, St. Louis, MO, U.S.A.) at 5 mg/kg body weight for the first 3 consecutive days of the week for 4 weeks. Vitamin B_{12} (Wako Pure Chemicals, Osaka, Japan) was administered intraperitoneally at 10 mg/kg body weight at the same time as DMN. After 4 weeks of treatment, the mice were anesthetized, and blood samples were taken from the orbital sinus. The animal experiments were conducted according to the ethical guidelines of the Osaka University Graduate School of Pharmaceutical Sciences.

Histological Analysis Liver specimens were fixed in 10% formaldehyde and embedded in paraffin. Sections were cut from the tissue blocks, mounted on slides, and stained with Elastica van Gieson (EG).

Assays Serum aspartate aminotransferase (AST) and alanine aminotransferase (ALT) levels were measured using an assay kit (Iatrozyme TA-Lq; Mitsubishi Kagaku Iatron Inc., Tokyo, Japan).

Reverse Transcription-Polymerase Chain Reaction (RT-PCR) The liver was excised and homogenized after removing the blood with phosphate-buffered saline. The total RNA was extracted from the liver homogenates using Sepasol-RNA I (Nacalai Tesque, Kyoto, Japan). The gene expression of α-smooth muscle actin (α-SMA) was analyzed by RT-PCR using the following primers: forward 5′-CAGGGAGTAATGGTTGGAAT-3′ and reverse 5′-CGTCGTATTCCTGTTTGCTGA-3′. Heat-shock protein 47 (HSP47) gene

* To whom correspondence should be addressed. e-mail: yagi@phs.osaka-u.ac.jp.

expression was analyzed using the following primers: forward 5′-CCATCGACAAGAACAGA-3′ and reverse 5′-TCATATTTCCCTTCCCCCCATC-3′. β-Actin gene expression was analyzed using the following primers: forward 5′-CATCCCCCAAAGTTCTAC-3′ and reverse 5′-CCAAAGCCTTCATACATC-3′. RT was performed using 1 μg of total RNA sample with the BcaBEST RNA PCR kit (Takara, Kyoto, Japan). The PCR conditions were: 1) 94 °C for 1 min; 2) 30 cycles of 30 s at 94 °C, 30 s at 55 °C, and 1 min at 72 °C; 3) 72 °C for 5 min.

Statistics The data were analyzed for statistical significance by Student's *t*-test.

RESULTS AND DISCUSSION

We examined the hepatoprotective effect of vitamin B_{12} on DMN-induced liver injury in mice. As shown in Fig. 1, after 4 weeks of DMN treatment, the activities of blood AST and ALT increased 2.9- and 3.3-fold, respectively, compared with controls, and the intraperitoneal administration of vitamin B_{12} significantly decreased the activities of AST and ALT. These results suggest that vitamin B_{12} suppresses the hepatic inflammation caused by the DMN treatment.

We next examined the effect of vitamin B_{12} administration on liver injury and fibrogenesis (Fig. 2). Liver sections were prepared after 4 weeks of DMN treatment and examined by EG staining. EG staining showed the significant accumulation of collagen fibrils after DMN treatment. This accumulation was clearly lower in DMN-treated mice given vitamin B_{12}. DMN bioactivation is thought to occur through the liver mixed-fuction oxidases (cytochrome P450 2E1).[10] The end result is the formation of toxic intermediates such as hydroxyl radicals, reactive oxygen intermediates.[11] Therefore, vitamin B_{12} appears to protect liver from the oxidation stress caused by DMN.

To confirm the antifibrotic effect of vitamin B_{12}, we next examined the gene expression of α-SMA and HSP47, which are markers of fibrosis, using RT-PCR analysis. As shown in Fig. 3, marked upregulation of the expression of the α-SMA and HSP47 genes was observed in the DMN-injured liver compared with the control liver. Therefore, although the liver damage was not fatal, the long-term liver injury caused inflammation and resulted in fibrosis. Vitamin B_{12} significantly

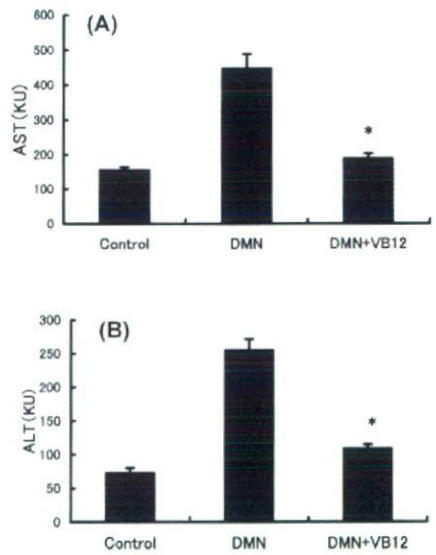

Fig. 1. Suppressive Effect of Vitamin B_{12} on Blood Transaminase Activities in DMN-Treated Mice

(A) AST, (B) ALT. DMN and vitamin B_{12} were injected intraperitoneally three times a week for 4 weeks. Values are the mean±S.D. (n=3 animals). *p<0.05, compared with DMN alone.

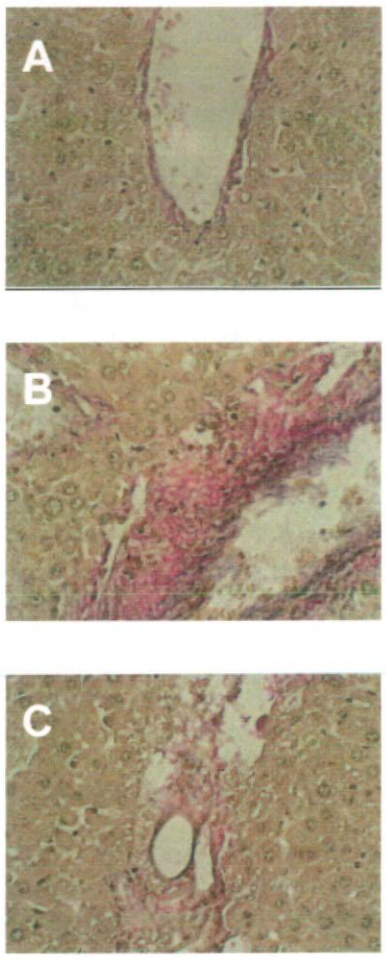

Fig. 2. Elastica van Gieson Staining for Collagen Fibrils

(A) Untreated control, (B) DMN treatment alone, (C) DMN and vitamin B_{12} treatment. Original magnification ×400.

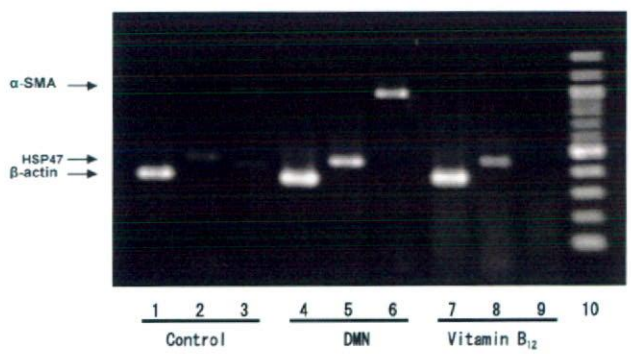

Fig. 3. RT-PCR Analysis of Gene Expression Related to Liver Fibrosis in DMN-Injured Mouse Liver

(Lanes 1, 4, 7) PCR products showing β-actin expression. (Lanes 2, 5, 8) HSP47 expression. (Lanes 3, 6, 9) α-SMA expression. Lane 10, molecular size markers.